1975

Petrogenesis of the Purcell Sill Glacier National Park Montana

Peter Francis Mejstrick
The University of Montana

PETROGENESIS OF THE PURCELL SILL
GLACIER NATIONAL PARK, MONTANA

by

Peter F. Mejstrick

A.B., Bowdoin College, 1971

Presented in partial fulfillment of the
requirements for the degree of

Master of Science

UNIVERSITY OF MONTANA

1975

Approved by:

Chairman, Board of Examiners

Dean, Graduate School

Date

ProQuest LLC.
789 East Eisenhower Parkway
P.O. Box 1346
Ann Arbor, MI 48106 - 1346

ABSTRACT

Mejstrick, Peter F. Geology

Petrogenesis of the Purcell Sill Glacier National Park, Montana

Director: Donald Hyndman

The Purcell Sill of Glacier National Park is a Precambrian alkaline olivine diabase that outcrops along the Continental Divide from the southern boundary of the park northward into Canada. The sill is marked by the assimilation and subsequent contamination by quartzite and dolomite xenoliths. Quartzite xenoliths added SiO_2 to the diabase and dolomite xenoliths added MgO and CO_2, and withdrew Al_2O_3 and SiO_2. Xenoliths rose in the sill in accordance with their densities to collect in a 'granophyric' hybrid zone. Chemical and petrographic data suggest that approximately 4 cubic meters of xenoliths were infused per 28 cubic meters of diabase.

TABLE OF CONTENTS

LIST OF TABLES

LIST OF FIGURES

INTRODUCTION

The Purcell Sill of Glacier National Park in northwestern Montana is one of many basaltic rocks included under the broad heading of the Purcell Suite. This grouping is extensively developed as sills, dikes, and lavas in the McGillivray, Galton and Purcell Ranges of British Columbia, and the Lewis and Livingston Ranges of Montana (Daly, 1912).

This particular sill was chosen for examination because of its extensive assimilation of xenoliths. The object of this report is to describe the inherent chemical, mineralogical, and petrographic transformations associated with these assimilation processes and thereby develop a detailed petrogenesis for this sill as well as a general model for similarly affected basaltic rocks.

Previous Work

Finlay (1902) was the first to reconnoiter the igneous geology in the area of Glacier National Park. His report includes outcrop relations of both intrusive and extrusive phases and their basic petrography.

The work by Daly (1912) on the geology north of the forty-ninth parallel provides a more detailed description. Whereas most of his discussion is based on the observations of the abundant igneous rocks of the Purcell Range in British Columbia, for which the regional suite is named, he provides petrogaphic descriptions of lavas, sills and dikes in the area of Glacier National Park and in adjacent Waterton National Park.

The general geology of Glacier National Park has been described by Ross (1959). However, little time was spent in the study of the sill, the report providing some outcrop locations and brief petrographic descriptions. Ross is responsible for the misnomer 'metagabbro' which is the common but misleading terminology for the rock in the park. A geologic map accompanies his paper but unfortunately the sill is incompletely and imprecisely mapped.

Hunt (1958) described the petrography of the Purcell Sill in the St. Mary region of British Columbia, his work overlapping into Waterton and Glacier National Parks. A more extensive study (Hunt, 1961) includes chemical analyses and a compilation of data for the province. This latter paper reports the age of the sill as 1100 X 10^6 years by K-Ar methods on an amphibole from the sill at Logan Pass.

General Geology

The Purcell Sill of the area outcrops from the northern edge of the Flathead National Forest northwestward through both Glacier and Waterton National Parks to beyond Yarrow Creek in British Columbia, about 30 miles north of the international border (Figure 1). Its exposures to the east and west are controlled by a broad syncline the axis of which trends in this northwesterly direction. The rocks within the area are of the Belt Supergroup and are nearly undisturbed and only locally folded or cut by minor steeply-dipping faults. A low-grade burial metamorphism is superimposed on all the rocks, the lower-most Altyn Limestone reaching the chlorite zone (Eslinger and Savin, 1973).

Information on geography, stratigraphy, structure and geomorphology of the area is contained in Ross (1959).

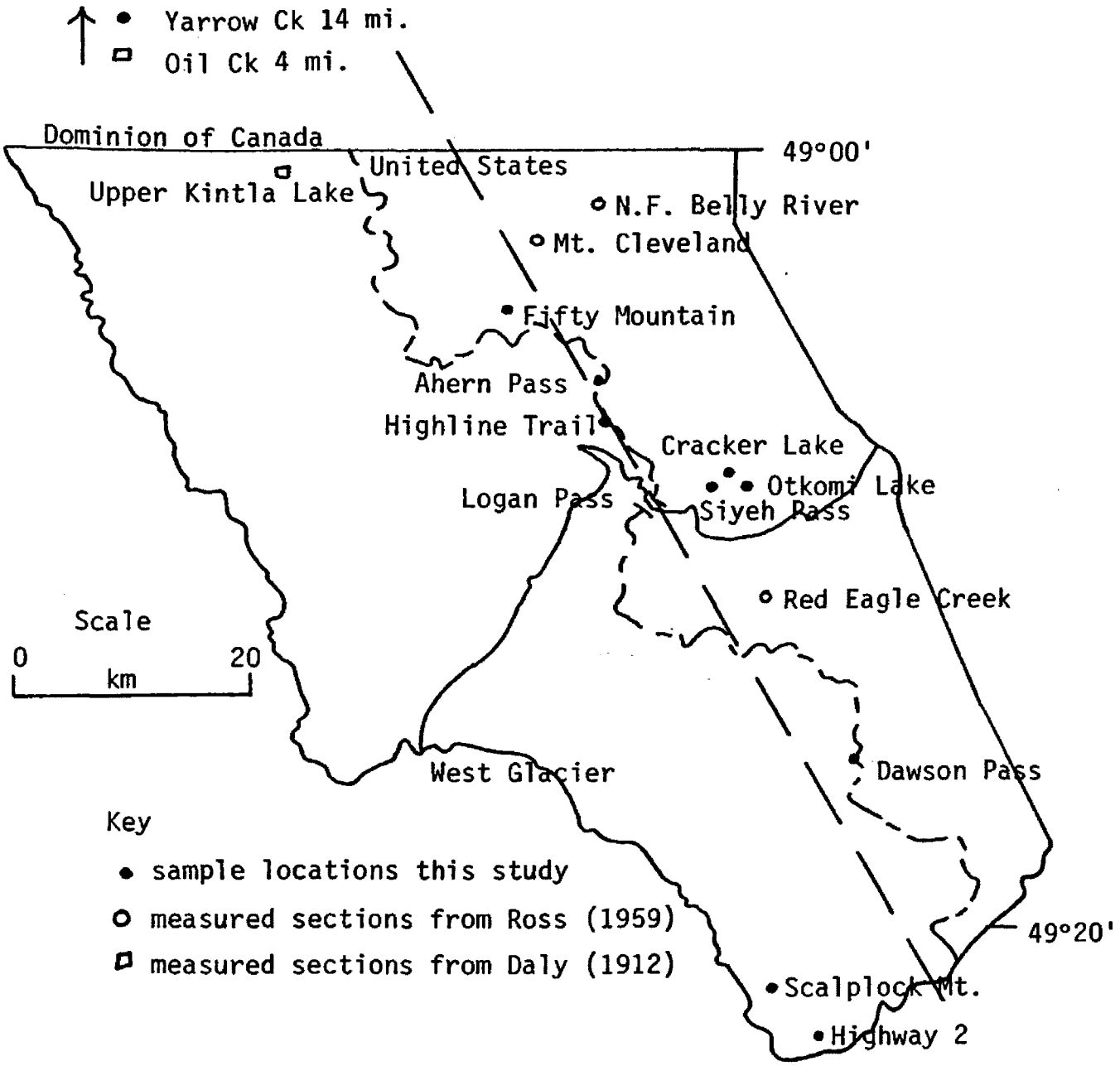

Figure 1. Index map of Glacier National Park with sample locations. A--A' line of cross section for Figure 2. Collection sites described in Appendix B.

CHAPTER II

FIELD RELATIONSHIPS OF THE PURCELL SILL

Intrusive Form

The Purcell Sill is a sheet-like intrusion of diabase with both lower and upper contacts mainly concordant with the Precambrian Siyeh Limestone. Major discordant breaks may be seen on the north side of the Garden Wall east of Swift Current Pass and on the north side of Mt. Cleveland where it turns upward as a dike for approximately 170 meters (Daly, 1912). Minor irregularities are more numerous at the top than at the base, generally occurring in the thicker sections, presumably near the loci of injection.

Thicknesses measured in this study and those by previous authors are shown in Figure 2. Data on the granophyric zone from this study is also included. It is evident that the thickest section is near Siyeh Pass, the sill thinning evenly in both a northwest and southwest direction. The data also suggest that the diabase thins to the northeast and southwest and therefore varies radially about a point near Siyeh Pass. Granophyric material correspondingly diminishes with the thickness of the diabase except where abnormal thicknesses have collected by up-dip migration. This phenomenon is most easily seen about one kilometer from Logan Pass above the Highline Trail. Viewed toward the northeast, the sill conforms to a stretched Z pattern with roughly 7 meters of granophyre at its upper edge and only isolated xenoliths where it begins its upward rise (see Figure 3).

Prominent dikes outcrop in a swarm between Rose Basin and Grinnell Glacier on the north side of the Garden Wall. Dikes trend north-

Table 1. Measured Sections of the Purcell Sill

SECTION	THICKNESS	GRANOPHYRE
Ahern Pass	26.8 m	4.0 m
Dawson Pass	26.8	4.0
Fifty Mt.	19.8	3.5
Highline Trail	28.6	4.9
Highway 2	9.2	trace
Mt. Cleveland[1]	19.6	n.d.
N.F. Belly River[1]	21.0	n.d.
Oil Creek[2]	15.2	n.d.
Red Eagle Creek[1]	27.4	n.d.
Scalplock Mt.	9.2	trace
Siyeh Pass	32.4	6.8
Upper Kintla Lake[2]	12.2	n.d.
Yarrow Creek	10.0	trace

[1] Data from Ross (1959).

[2] Data from Daly (1912).

n.d. Not determined.

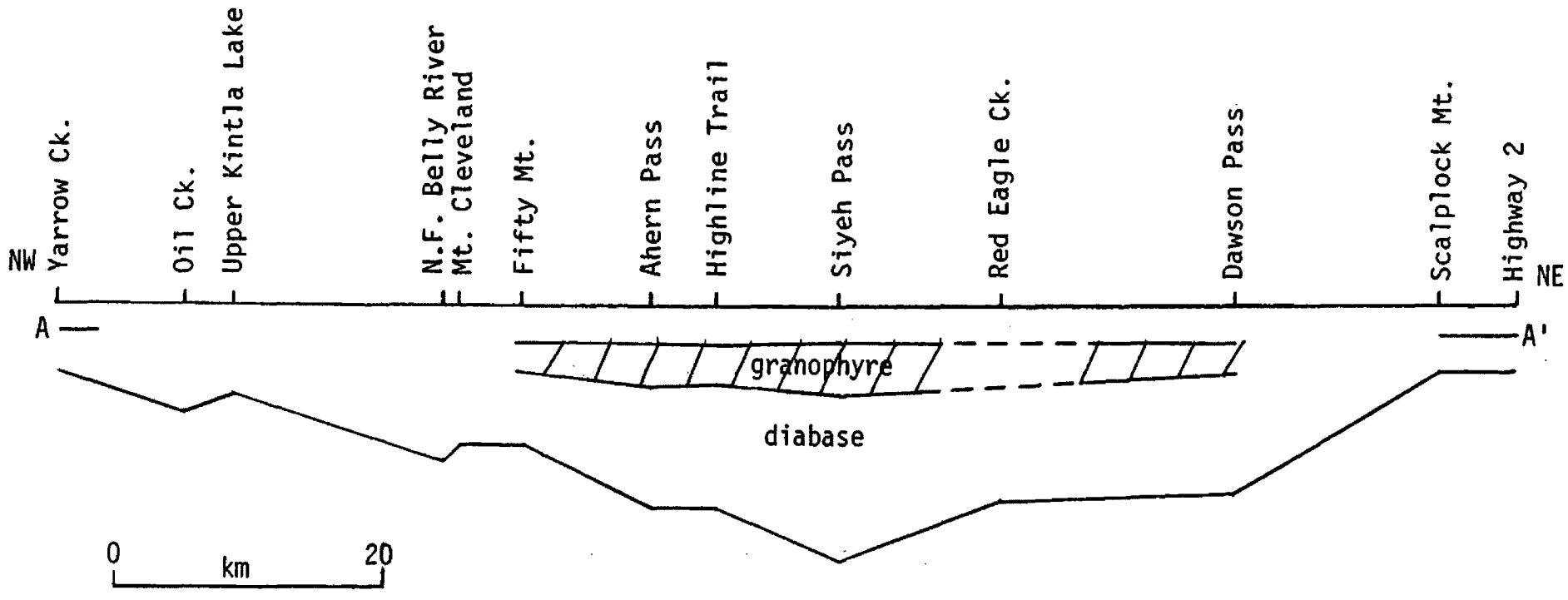

vertical exaggeration 520x

Figure 2. Cross section of Purcell Sill. Measured data plotted from normal to line A--A' Figure 1.

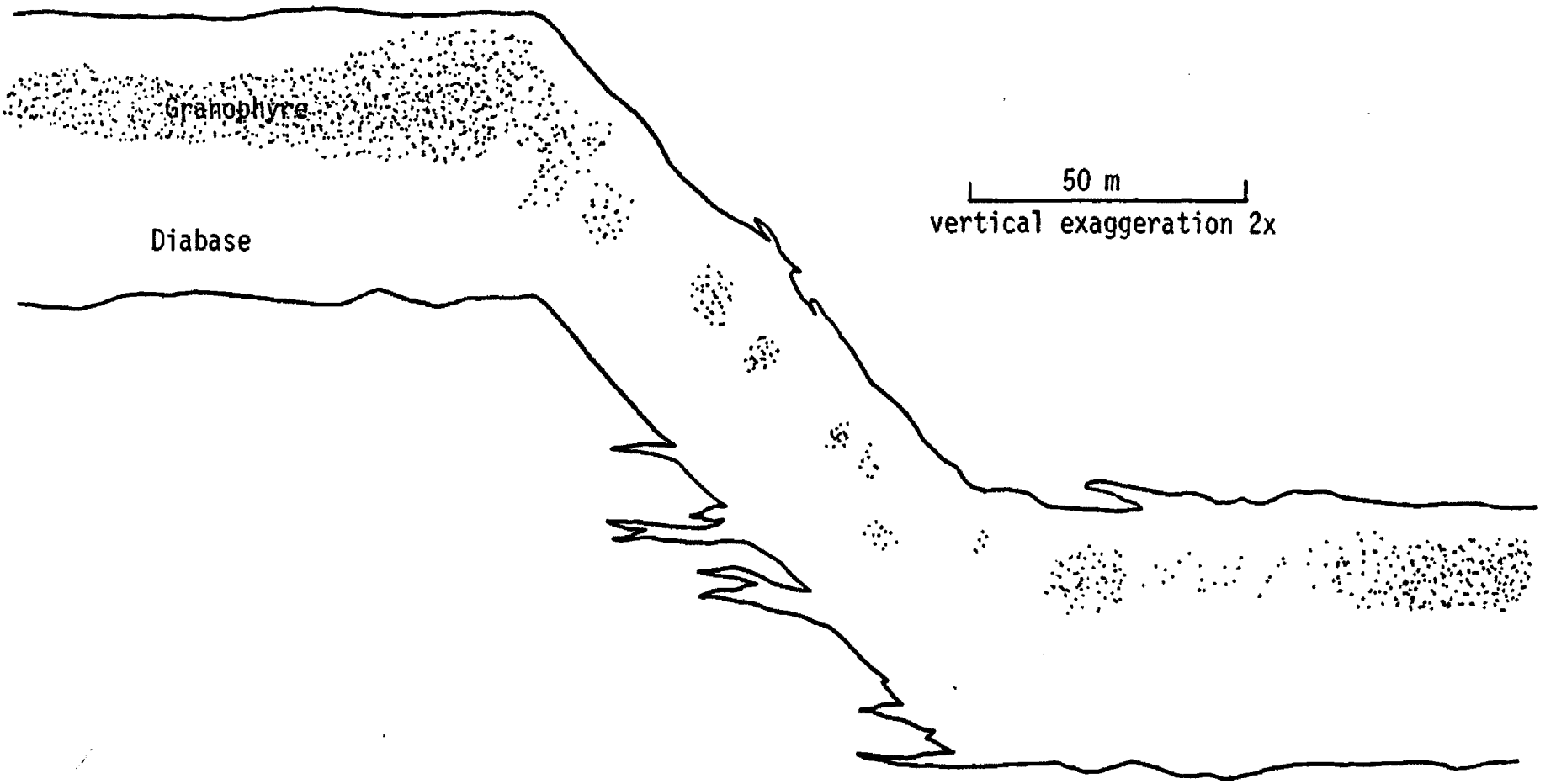

Figure 3. Schematic view northeast along Highline Trail near Logan Pass showing up-dip migration of xenoliths. Isolated xenoliths may be seen in trail exposures.

west and dip steeply. Thinner associated dikes outcrop throughout the park but appear to be unimportant in the genesis of the sill.

Contacts

Upper and lower contacts of the sill are remarkably sharp, and there is no hint of diabase aggression or assimilation of the country rock, the Siyeh Limestone. In handspecimen the chilled diabase is fine grained and black, or, with greater deuteric alteration, dark gray-green. Margins and apophyses are locally glassy and support randomly oriented phenocrysts of titanaugite. Grain size rapidly increases inward for 120 to 150 cm, where groundmass minerals are visible. The diabase immediately adjacent to the limestone is intensely fractured due to late readjustments during cooling.

The Siyeh Limestone is metamorphosed to marble and bleached white for 6 to 9 meters from the sill. The fine structure of stromatolites and molar tooth fragments are preserved, although the rock is completely recrystallized. No mineralogical changes are associated with this process and the rock remains a combination of calcite and quartz. Contact metamorphism is locally variable in extent but less where the sill is thinner.

The Siyeh Limestone has not undergone deformation from the intrusion of the sill. This is in marked contrast to the highly distorted country rock at the Cracker Lake and Otokomi Lake dike exposures. Here the Grinnell argillites are metamorphosed and folded for up to 6 meters from the contacts. Both dikes are considered feeders to the sill.

Jointing

Columnar jointing occurs at all levels of the sill but is classically developed at the contacts where cross sections measure 30 to 60 cm in diameter. Cross joints are subparallel, well defined, and randomly spaced.

An obvious deflection in this fracture pattern occurs at the juncture between the columnar joints of the upper diabase and the granophyre. Joints in the upper diabase are sharp and regular whereas those of the granophyre are either highly irregular or completely absent. In many cases, it is possible to follow this change in an individual column which is distinct in the diabase but curves and becomes less defined upon entering the granophyre. Spry (1961) suggests that this difference in joint patterns is a result of differential cooling. As discussed in chapter VII, the granophyre was probably the last section of the sill to consolidate.

Late Veins

Joints are commonly filled with a residual material composed of radiating epidote with minor diopsidic pyroxene and quartz. The largest of these veins observed measured 3 cm in width, but the majority are on the order 5 mm. They typically extend the length of the joint, up to 5 meters, or gradually thin and disappear. The diabase adjacent to the vein is discolored with a greenish tint of saussuritized plagioclase, the thickness of the alteration halo depending on that of the vein. Veins are concentrated in both upper and lower contact zones. Later readjustment of joint blocks has converted the epidote to a slickensided chlorite.

A rare second type of vein is composed of pink alkali feldspar, quartz and epidote. Such dikelets do not follow preexisting fractures but drift irregularly throughout the diabase in sharp contact with the host rock. Their appearance recalls lenses of alkali feldspar and quartz which are 'sweated out' of high grade regional metamorphic rocks, and their origin may be more akin to a late pegmatic differentiate than an injected residuum.

Xenolith Distribution and the Granophyric Zone

The unique character of the sill appears to have resulted from the assimilation of foreign material. Two types of fragments dominate: an albite-alkali feldspar-quartz or quartzite type, and a calcite-epidote or dolomite type, the fragments of each occurring in nearly the same numbers. Micaceous inclusions are rare, identified solely in the dike at Cracker Lake, and because of their lesser numbers have not affected the petrogenesis of the sill.

Xenoliths are evident in all outcrops. Sizes average less than 20 cm and range from less than 2 cm to spherical masses with diameters greater than 120 cm. The larger of these are of the dolomite variety. Xenoliths are rendered doubly conspicuous by either their pink alkali feldspar or green epidote color against the dark diabase.

Dike exposures afford the possibility of establishing the genetic sequence of progressive assimilation. At Otokomi Lake, where only dolomite xenoliths are present, three stages of development are apparent (Figure 3). The primary, or stage I inclusion, has a core of crystalline calcite or of massive quartz surrounded by splayed and embayed epidote. Stage II is exemplified by cores of massive

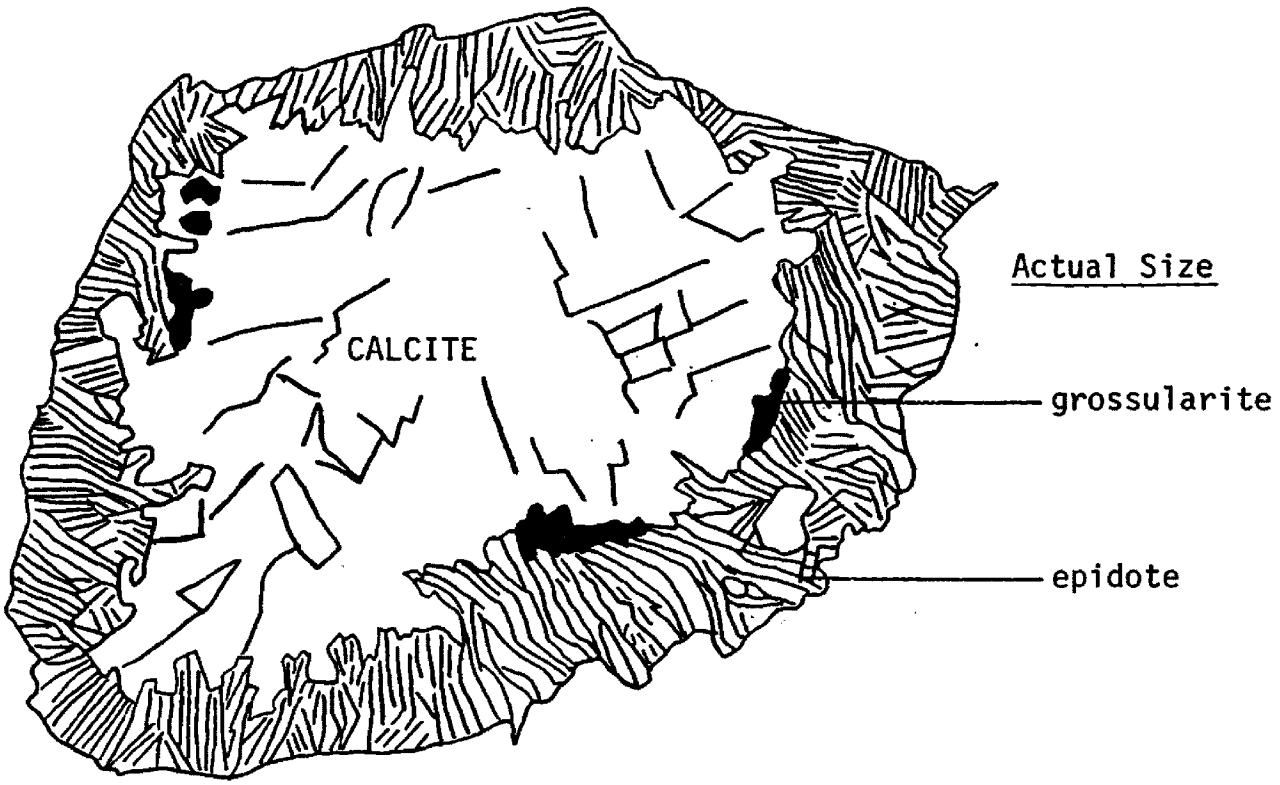

Figure 4a. Handspecimen sketch of stage I dolomite xenolith enclosed in diabase.

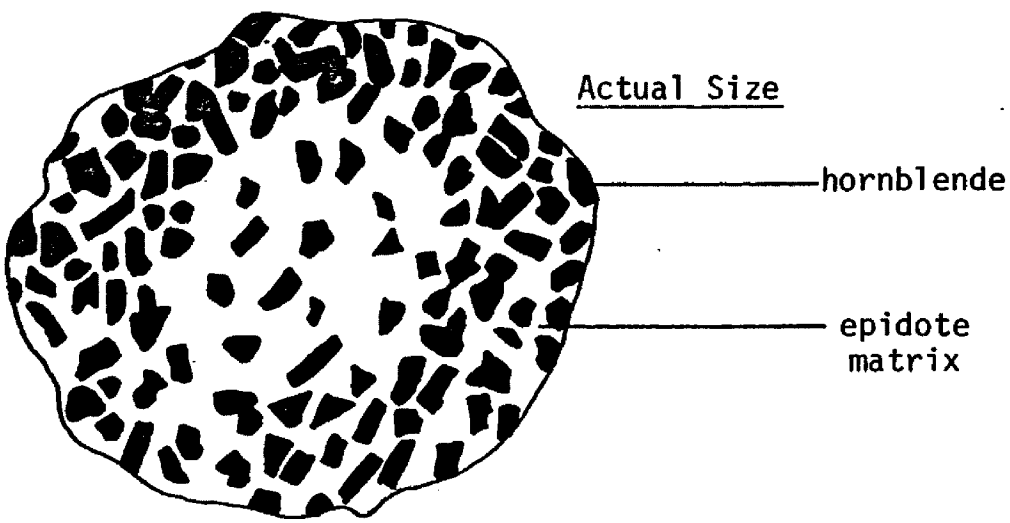

Figure 4b. Handspecimen sketch of stage II dolomite xenolith enclosed in diabase. The density of hornblende crystals increases toward the margins.

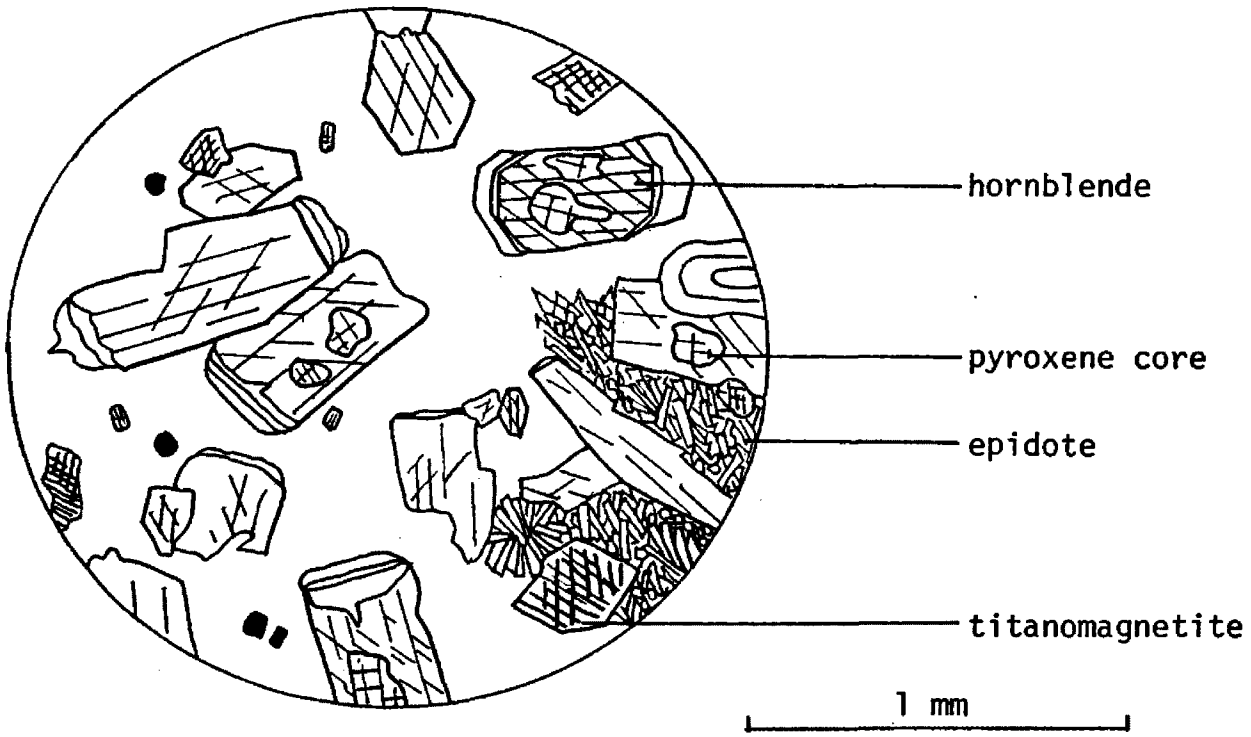

Figure 4c. Thin-section sketch of stage II dolomite xenolith. Hornblende contains cores of calcic pyroxene in a matrix of epidote. Retrograde rims of pale tremolite surround hornblende. Clear areas epidote matrix.

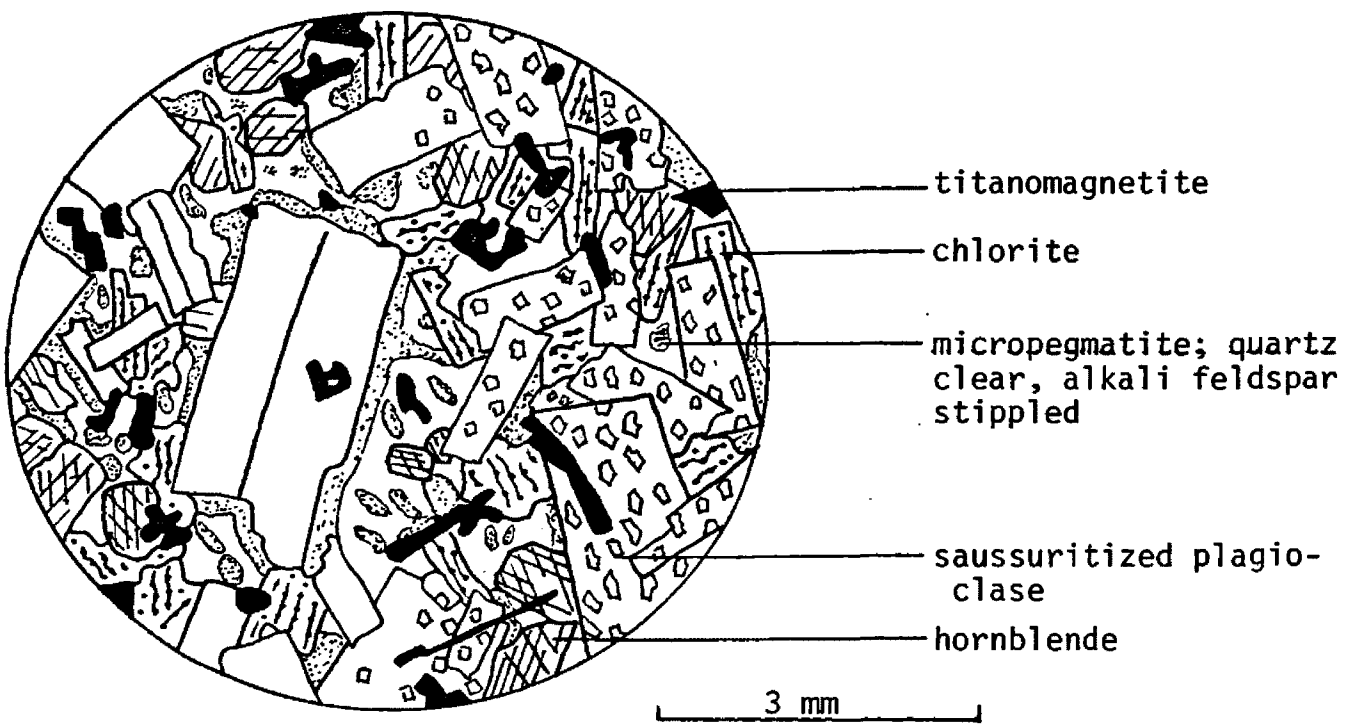

Figure 4d. North-south contact between stage III dolomite xenolith and diabase. Plagioclase on right half, epidote, on left half, sericite and clay minerals.

epidote grading outward into epidote with fibrous amphibole that increases in amount toward distinct contacts with the diabase. The rock is commonly speckled white by alkali feldspar and quartz. In thin section epidote typically forms small angular grains in imperfect radiating patterns and abuts euhedral hornblende up to 2 mm in length (Figure 3c). Hornblende grains exhibit retrograde zones which become wider and more numerous toward the edge of the xenolith. Hornblendes, especially those in the center of the xenolith, have cores of diopside, ($2V_Z$ = 59°). Alkali feldspar and quartz are in graphic intergrowths and opaques are irregularly shaped and scattered throughout the rock. Modal analysis (1000 grains) on an alkali feldspar and quartz free rock gave 62% epidote, 27% hornblende, 9% pyroxene, and 2% opaques. The most advanced stage, III, is characteristic of those xenoliths found within the sill. They occur as spherical pod-like structures of granular epidote (after plagioclase) and evenly distributed amphibole with patches of pink alkali feldspar and quartz. Many of the textures associated with the adjacent diabase are evident within the xenolith (Figure 3d). The essential difference between the pod and the diabase is the greater hydrothermal alteration within the pod. Alteration is manifested as saussuritization of plagioclase laths by minutely interlocking grains of epidote and by the conversion of hornblende and pyroxenes to chlorite. Modal analysis of the inclusion gives 55% plagioclase (now epidote); 20% micropegmatite; 19% hornblende, pyroxene and chlorite; and 6% Fe-Ti oxides. The adjacent 5 cm of diabase is similar with 53% plagioclase; 14% micropegmatite; 26% hornblende, pyroxene, and chlorite; and 7% Fe-Ti oxides. If this contaminated

diabase is compared to the normal diabase (Table 4a, 4b) it is evident that the xenolith has affected the diabase in such a way as to increase the plagioclase and alkali feldspar-quartz content and to decrease the ferromagnesian minerals. Likewise, when stage I or II xenoliths are compared to the stage III type, gross changes in composition are indicated. It is believed that large scale exchanges between dolomite xenoliths and diabase are a controlling factor in the petrogenesis of the sill. This concept is further developed in chapter VI.

Progressive modifications in the quartzite xenoliths are less certain. Two types occur in the Cracker Lake dike, between which there is a continuum of composition. Gray inclusions are composed of albite and quartz, and pink inclusions of albite, alkali feldspar and quartz. Both contain variable amounts of interstitial calcite and pseudomorphs of pyroxene altered to epidote and chlorite. The inclusions have been recrystallized as attested by their sutured grain boundaries (Figure 5). The composition of these xenoliths suggests a limey sandstone as a parent. Since extensive units of quartzite composition are not exposed in the sections of the Belt Supergroup in this area, it is presumed that these represent either basement rocks, or unexposed units below the Altyn or Waterton Formations.

Quartzite xenoliths show little tendency toward disequilibrium within the magma and only in rare cases have margins of glass or reaction rims of pyroxene developed adjacent to the xenolith. Diffusion bands, however, are common and demonstrate exchange between diabase and inclusion. In these halos the outer edge of the xenolith is typically discolored green by the alteration products of epidote

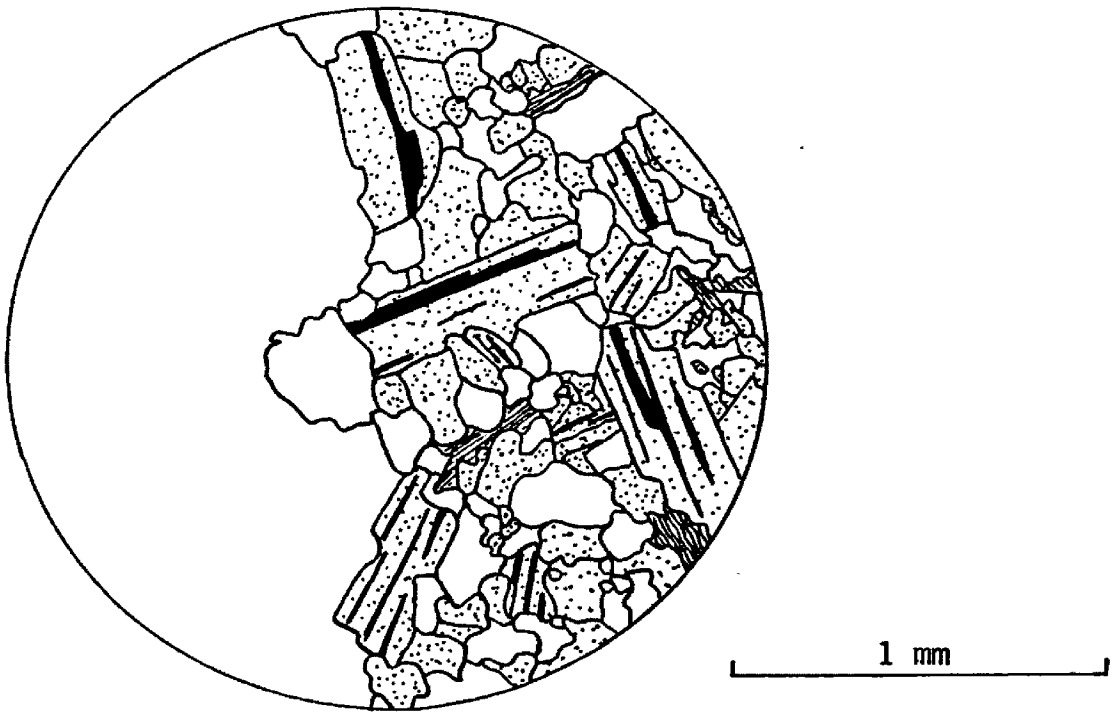

Figure 5. Sutured grain boundaries in a quartz-albite xenolith. Quartz clear; albite stippled. Clear area similar.

and chlorite whereas the diabase is mottled by quartz and pink alkali feldspar which continues outward for 5 cm or more before grading into normal diabase.

It is not possible to trace the behavior of these xenoliths as in the case of the dolomite type, as intermediate products are absent from the lower diabase of the sill. They are subsequently encountered in the granophyric zone, and at this level they no longer retain characteristics that may be attributed simply to quartzite-diabase interaction. A description of the rock is given in the next chapter.

Xenoliths are virtually absent from the chill margins and scarce in the lower diabase which makes up the bulk of the sill (Figure 6). Epidote pods occur in the lower 3 to 5 meters but are prominent only 1 to 3 meters below the granophyre. Along a traverse upward toward the base of this hybrid zone, quartzite xenoliths appear and both gradually become more abundant to a point about 1 meter below it. The xenolith population increases abruptly within this 1 meter interval and terminates in a homogeneous granophyric horizon.

The granophyric zone itself is a conglomeration of xenoliths, and is not a true granophyre in the sense of a product of a differentiated magma. This is not obvious in its lowermost portions where individual inclusions lack boundaries and blend together. The rock is a hybrid of xenoliths and diabase with pink and green patches, long fibrous amphiboles, stubby pyroxenes and stout plagioclase laths. There are numerous miarolitic cavities. In the upper portions this homogeneity is not as pronounced and large block or combinations of inclusions are separated by pink speckled diabase similar to that found surrounding isolated xenoliths. The granophyre gradually gives way upward to

diabase through a diffuse transition zone.

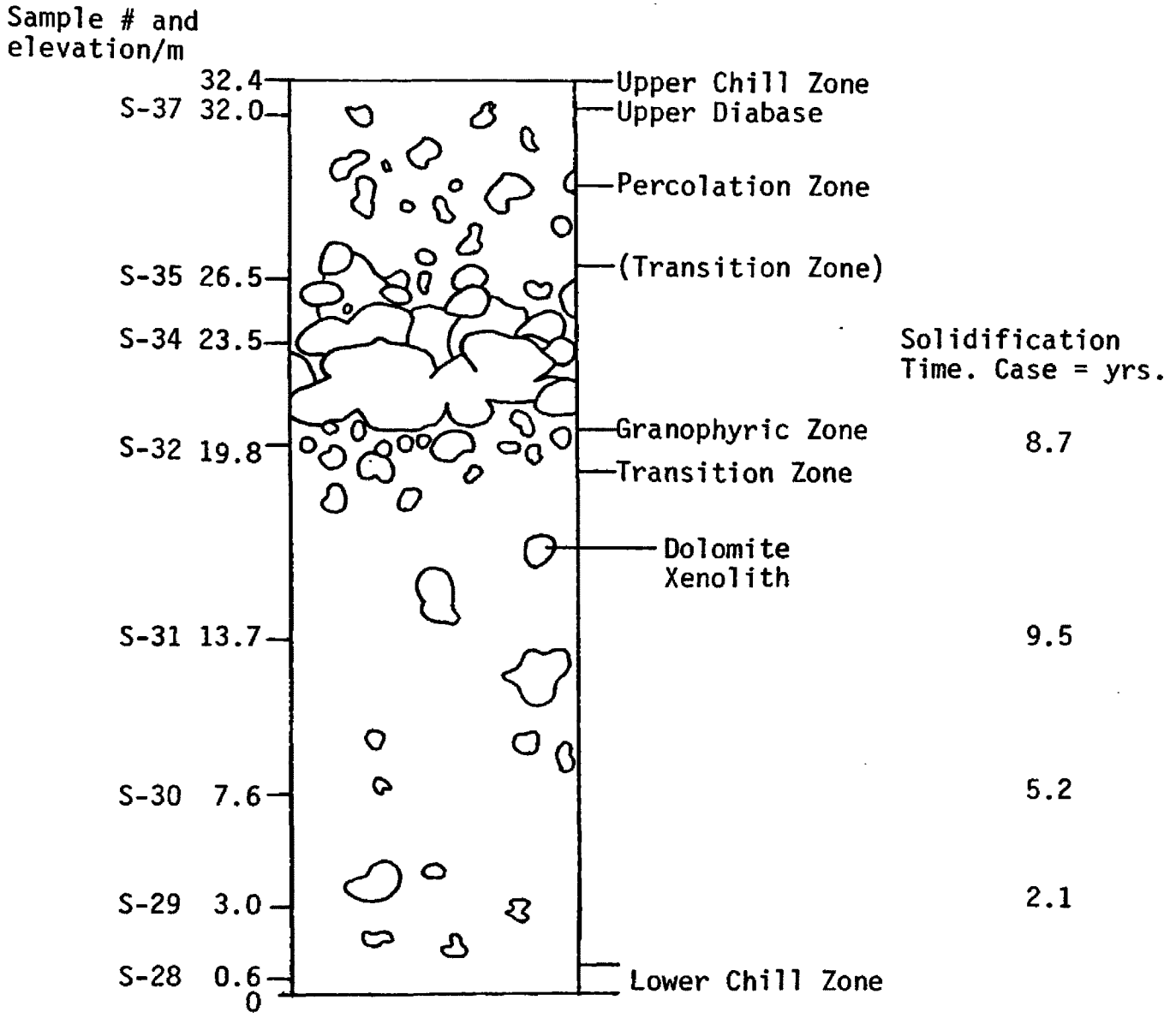

Figure 6. Columnar section of the Purcell Sill, at Siyeh Pass. See Appendix A for Cooling History.

CHAPTER III

PETROGRAPHY

The petrography of the Purcell Sill is conveniently discussed by consideration of three gradational rock types. From the base upward these are termed the chilled diabase, the lower diabase, and the granophyre. Their distribution is depicted in Figure 6. The lower diabase comprises the bulk of the sill followed in amount by the granophyre, and then the chilled diabase.

Chilled Diabase

The chill zone extends about 120 cm from either top or bottom contact. Inward of 120 cm, grain size rapidly increases and crystal habits and mineralogy become typical of the lower diabase. Average thin section length of the opaques shows the greatest measure for comparison with .05 mm in this zone compared to .18 mm in the overlying diabase. There are no differences petrographically or chemically between samples from either margin.

Samples within the chill zone show extensive deuteric alteration. Plagioclase is largely altered to sericite or fuzzy kaolinite, so much so that individual grain boundaries are generally no longer evident. Titanaugites are corroded with rims of brown hornblende, which in more advanced stages, have gone over to indistinct biotite or a brownish green, poorly crystalline chlorite. Opaque needles are converted to leucoxene.

Titanaugite phenocrysts typically show hour-glass zoning with superimposed concentric zoning of alternating brown ($2V_z$ = 58°) and and clear ($2V_z$ = 42°) zones. Cores are characteristically brown.

Phenrocrysts tend to form glomeroporphyritic aggregates of three or more crystals, many of which are fractured or chipped into irregular grains exhibiting undulose extinction. Pyroxenes in the groundmass are generally anhedral in aggregates of up to 100 or more grains although euhedral edges are locally developed. Much of this groundmass pyroxene is altered or replaced by hornblende. The hornblende commonly occurs as indistinct brownish green crystals with no apparent cleavage and irregularly rims or has completely replaced both phenocrysts and groundmass crystals. A primary, rich dark brown hornblende with perfect cleavage and subhedral habit also mantles and partially resorbs pyroxenes, or occurs as independent grains. Rimming the brown hornblende is a green phase that shows well-defined cleavage and euhedral edges and is thought to have crystallized directly from the melt.

Titanomagnetite is uniformly dispersed in skeletal shapes composed of minute euhedral trains of cubes or as single octahedra.

Other minerals are rare; of these interstitial intergrowth of anhedral alkali feldspar and quartz are the most common. They typically occur together in patches although alkali feldspar may occur as independent grains. A few grains of anhedral epidote and calcite have crystallized along with this interstitial material.

Diabase

The diabase displays subophitic to ophitic textures instead of the holocrystalline, intergranular nature of the margins. All groundmass minerals are coarser, with the maximum reached near the 15 meter level in the Siyeh Pass section. Orthopyroxene is an exception and is discussed in Chapter V.

Alteration is less extreme than in the chill zone, although it remains most obvious. Plagioclase is converted to sericite, chalky combinations of clay minerals or rarely granular epidote. Outlines may remain, revealing tabular crystals. Edges subject to residual fluids were resorbed and crystallized to alkali feldspar especially toward the top of the unit. Pyroxenes are randomly altered to chlorite, either partially or wholly. Their aggregate habit is maintained in all reaches of the lower diabase. Clinopyroxene and Te-Fi oxides are intergrown and resemble the subophitic fabric of plagioclase and pyroxene. In many cases the grains of titanomagnetite exsolved criss-cross ilmenite which in turn was replaced by leuxocene. Alkali feldspar is turbid and in graphic intergrowths with quartz. Figure 7 is a representative thin-section sketch of the textures in the diabase.

The above relations provide the basis for the order of crystallization of the major minerals. Plagioclase and clinopyroxene must have crystallized eutectically followed closely and in part by opaques. Primary hornblende formed after the clinopyroxene had ceased to crystallize and was in turn rimmed with primary green hornblende. Biotite in the upper sections maintains an equivalent position to the brown hornblende. Alkali feldspar and quartz, along with epidote and calcite crystallized in the interstitial sites.

Although textures are similar throughout this zone, there are significant modal variations (Figure 11, Table 4a, 4b). The bronzite shows the most change, increasing from 2 to almost 11 percent upwards. It occurs as euhedral blocky crystals and commonly contains randomly oriented rounded blebs of groundmass pryoxenes. Textures such as in

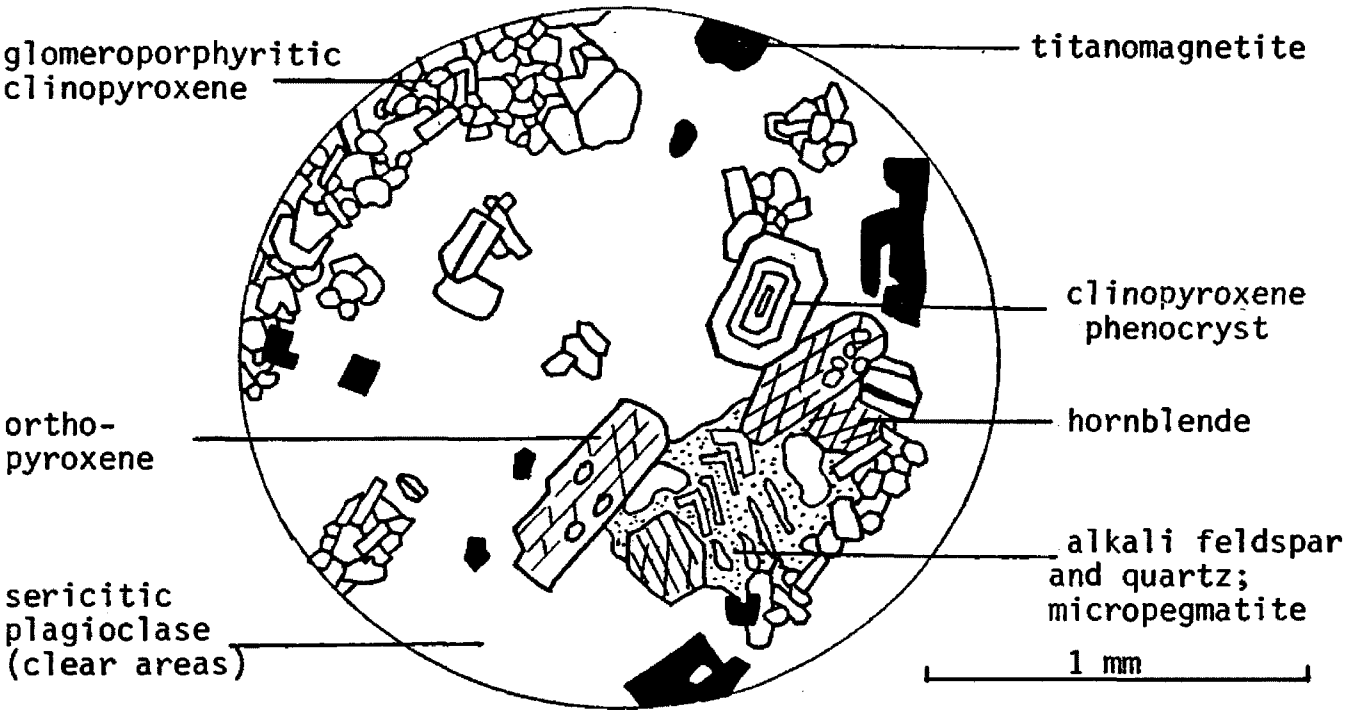

Figure 7. Texture of the diabase. Note glomeroporphyritic clinopyroxene, and development of hornblende proximal to micropegmatite. Crystal outlines of plagioclase are no longer visible because of turbid alteration.

Figure 8, where a clinopyroxene abuts an orthopyroxene with the included portion of the clinopyroxene rounded but the excluded part euhedral, point to a poikilitic origin for the clinopyroxene. It is thought that the included clinopyroxenes were inherited from poikilitic olivine, the olivine molecule reacting with free quartz in the magma to give orthopyroxene. Although the exact status of the orthopyroxene in the crystallization order is uncertain, it is definitely later than the clinopyroxene.

Granophyre

There is little petrographic similarity between the diabase and the granophyre. In the granophyre, coarse graphic texture dominates which has resulted from the increase in amount of interstitial alkali feldspar and quartz. Large tabular plagioclase is corroded by alkali feldspar where adjacent to these areas. A sector-zoned clinopyroxene appears as a stable ferromagnesian phase in place of the groundmass pyroxenes and orthopyroxenes typical of the diabase. It no longer maintains its eutectic relationship with plagioclase but occurs as stubby euhedral crystals. Remnant orthopyroxene is rare. Hornblende retains its character but forms larger, more euhedral crystals. Figure 8 is representative of the granophyre fabric. Replacement textures are similar to other portions of the sill. More chlorite, secondary biotite and hornblende is associated with the breakdown of the primary ferromagnesian minerals but plagioclase is less altered.

Calcite and epidote, two minor but petrogenically important phases, appear in a manner reminiscent of the epidote xenoliths. Calcite is irregularly rounded and embayed by crudely acicular epidote. They are clearly late and imbedded in a matrix of alkali feldspar and quartz.

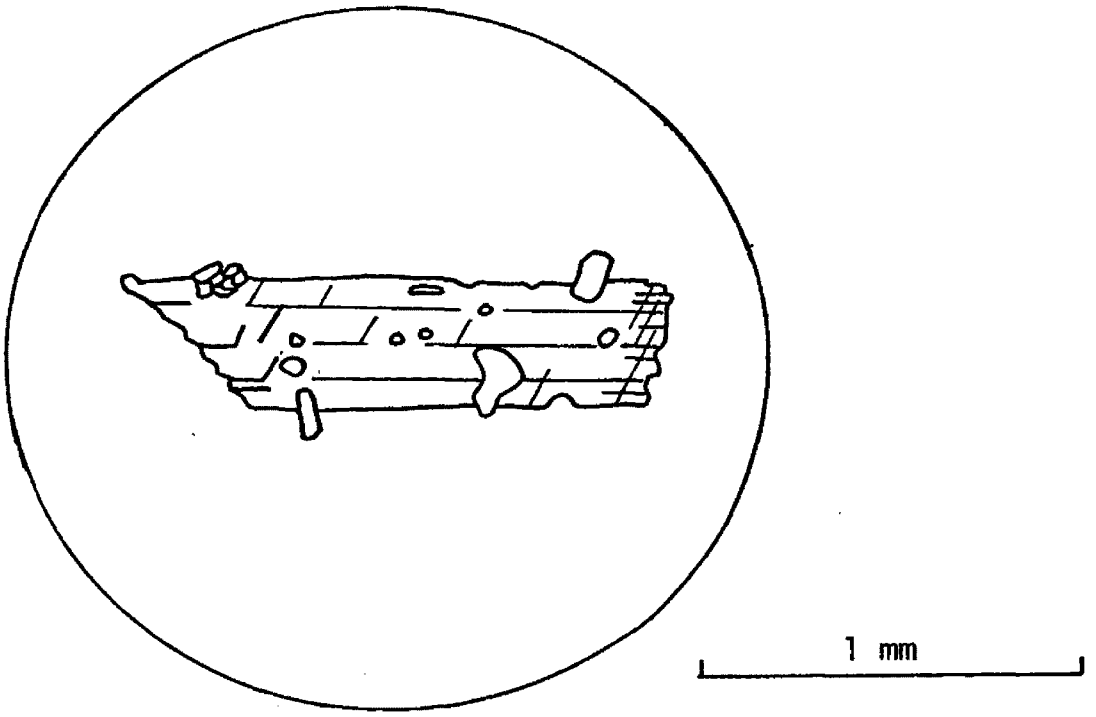

Figure 8. Orthopyroxene crystal with poikilitic clinopyroxene. Portions of clinopyroxene outside the orthopyroxene exhibit euhedral forms.

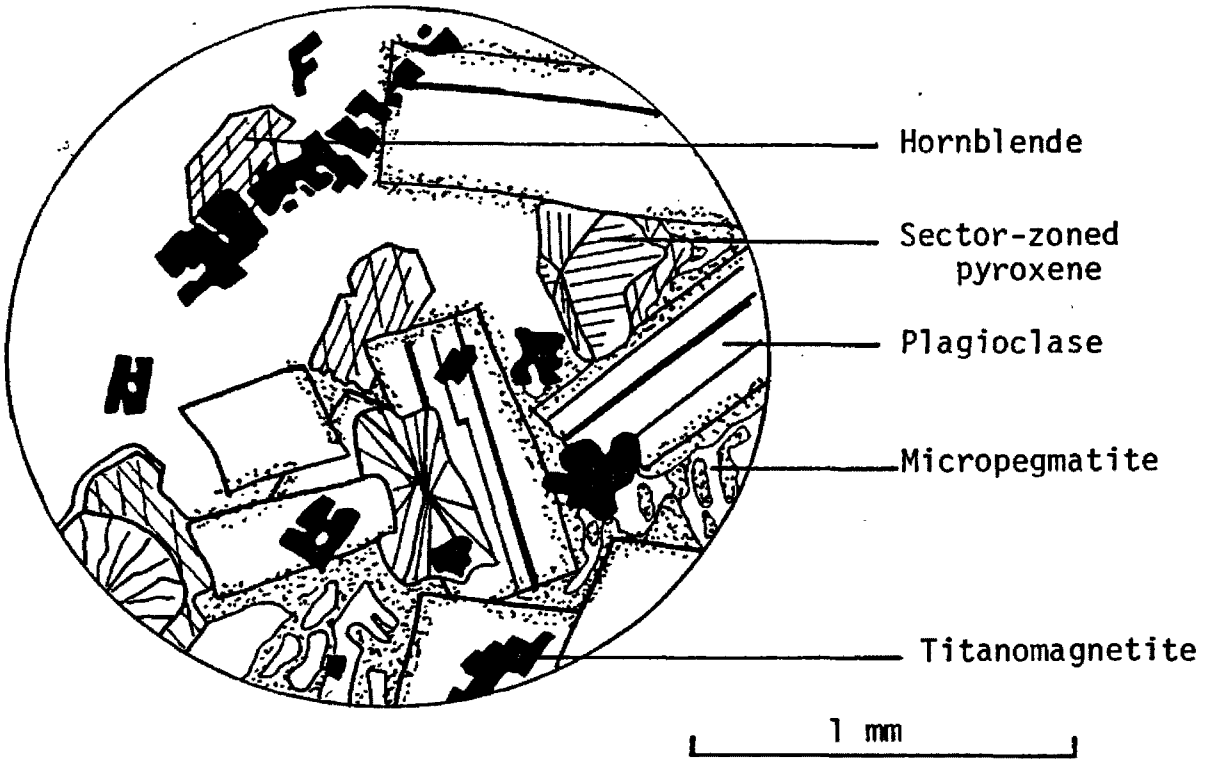

Figure 9. Texture of the granophyric zone. Hornblende partially rims and resorbs sector-zoned pyroxenes. The edges of plagioclase laths are resorbed by alkali feldspar. Clear area similar.

CHAPTER IV

DESCRIPTIVE MINERALOGY

Plagioclase and pyroxenes are the main minerals in the Purcell Sill, comprising close to 70% of the rock. Important minor constituents include alkali feldspar, quartz, hornblende, and Fe-Ti opaque minerals. Biotite is a minor accessory in the upper sections of the lower diabase whereas apatite, sphene, calcite, and pyrite occur at all levels. Deuteric action has altered some mineral groups and therefore descriptions of the resulting products are included. It is only by their recognition that the complete primary mineralogy can be deduced.

Plagioclase

Plagioclase is intensely altered throughout the sill. In fact, its conversion to sericite and submicroscopic clay minerals has in many cases proceeded so far as to obscure textural relationships. Twinning, where present, appears ghost-like beneath a cover of secondary minerals. Cleavages are no longer visible.

Several universal stage measurements by the method described by Slemmons (1962) were made on the crystals in order to determine their composition. Thin sections were investigated from the lower diabase at Dawson Pass and Ahern Pass. All contained plagioclase of an average composition of An_{34}. Hunt (1958) reports An_{35} as the most calcic composition he observed for the sill in this region. Ross (1959) however reports that the sill plagioclase is zoned with a range in composition of An_{75} at the core to An_{25} at the margins, and Daly (1912) mentions that the sill near Upper Kintla Lake contains labradorite. Labradorite

is typical for rocks of diabase affinities and therefore is probably the composition of the primary plagioclase in the Purcell Sill.

Clinopyroxene

Clinopyroxene is present as phenocrysts and in the groundmass of the diabase. Phenocrysts have conspicuous hour-glass zoning upon which concentric zoning may be superimposed. Optic axial angle ($2V_z$ = 59°), strong dispersion, and the hour-glass zoning infer a titaniferrous variety. Groundmass clinopyroxenes are generally subhedral to euhedral with simple twinning common on (010) and parting along (100). Surface irregularities and alteration give a brownish tinge to the otherwise colorless grains. All groundmass pyroxenes show strong dispersion at extinction and are therefore probably titaniferrous. Clinopyroxenes alter to chlorite with minute granules of sphene exsolved along internal fractures and the (100) parting.

Estimates of chemical composition were obtained by refractive index and optic angle. Attempts at separation proved futile because of irregular alteration and replacement rims of hornblende. Data is plotted on the standard pyroxene diagram (Figure 11). The compositions listed are only estimates, neglecting the effects of minor element substitution, especially titanium, however the trends are internally consistent and distinctive and may therefore provide information on the petrogenesis of the sill.

Crystallization of the Ca-rich pyroxene, to at least the 8 meter level, follows a normal path for alkaline olivine basalts in which Ca and Mg are progressively replaced by Fe (Wilkinson, 1956). At higher levels the trend abruptly reverses with Mg increasing and substituting

for Fe toward the top of the lower diabase. Approximately 7 mole % Ca is lost in this conversion, but for the remaining 13 meters of the lower diabase it is essentially constant.

Orthopyroxene

Orthopyroxene crystallizes as relatively large 0.7 mm euhedral grains with weak pleochroism. Crystals are poikilitic, enclosing small rounded groundmass titanaugites. Compositional data from Siyeh Pass are plotted in Figure 11. Optical properties vary within a given slide or oil mount. Samples below S-31, or a level of 14 meters, are completely altered to chlorite and talc, precluding compositional determinations.

Data from S-31 and S-32 demonstrate a similar reversal from normal basaltic crystallization. Again, the more 'fractionated' orthopyroxene is higher in Mg and lower in Fe than its predecessor.

Olivine

Olivine pseudomorphs were identified in the chill margin of the Otokomi Lake dike and in the diabase of the Dawson Pass and Highline Trail sections. The olivine occurs as subrounded grains altered to a drab olive brown product surrounded by a fringe of magnetite granules which in turn is mantled by chlorite. The chlorite represents an orthopyroxene which formed by a reaction such as:

$$SiO_2 + Mg_2SiO_4 \rightarrow 2MgSiO_3.$$

In some cases bronzite psuedomorphs contain cores of indistinct chlorite (?) not in optical continuity with the surrounding chlorite. These are believed to be remnant and non-resorbed olivine.

It is difficult to estimate the amount of olivine that was present in the uncontaminated magma. Hunt states (1958, 1961) that 2% of the sill near Logan Pass is composed of pseudomorphs after olivine. I examined similar specimens but cannot confirm his identification. Assimilation of quartzite apparently preceded injection since olivine is as sporadic in the chill margins as it is in the remainder of the diabase.

Hornblende

Hornblende occurs as a primary and a secondary mineral. Primary hornblende is brown and pleochroic with γ, bronze brown $>\beta$, pale brown $>\alpha$, pale yellow. It is characteristically subhedral but euhedral faces may develop where it abuts micropegmatite. Crystal size is relatively large, ranging up to 1.3 mm. A second variety of primary hornblende is green with a pleochroic scheme of γ, olive green $>\beta$, light green $>\alpha$, pale green, and regularly mantles the brown form. These outer zones become wider in the upper portions of the diabase.

No data were determined on hornblende. Hunt (1961) reports optical measurements on the brown variety as x = 1.660, y = 1.674, and z = 1.677 with a $2V_x = 50°$ and a $C\Lambda Z$ of 15°, and for the green variety as x = 1.656, y = 1.668, and z = 1.674 with a $2V_x = 70°$ and a $C\Lambda Z$ of 14° on a sample from the base of the sill near Logan Pass.

Secondary hornblende after pyroxene and primary hornblende are prominent in the chill margins and locally developed in the lower parts of the diabase where volatiles apparently were concentrated. It is pale green in color, resembling uralite.

Opaque Minerals

The majority of the oxides are ilmenite and titanomagnetite. In the latter exsolution and alteration of ilmenite to leucoxene produces a patchwork design on the grains. Common forms are needles at the margins and euhedral cubes, jagged skeletal rods and variable subhedra or anhedra in the more slowly cooled portions. Interpenetration with clinopyroxenes suggest that the opaques crystallized early and continuously.

A few small pyrite cubes or anhedra are evenly dispersed throughout the diabase. They are commonly altered to hematite.

Micropegmatite

Alkali feldspar and quartz comprise a micrographic interstitial intergrowth throughout the sill. Anhedral alkali feldspar or quartz occur rarely as independent grains. In thin section akalki feldspar is recognized by a turbid alteration to clay minerals, whereas adjacent quartz is clear. In the granophyre and other sections of the sill affected by contamination, the alkali feldspar mantles partially resorbed plagioclase, and in these cases is pink in handspecimen because of exsolved Fe^{+3} in the form of hematite (Ernst, 1960).

Biotite

Primary biotite is limited to the upper sections of the lower diabase. It is euhedral to subhedral in habit with a pleochroic scheme of γ, reddish brown $>\beta$, light brown $>\alpha$, yellow brown. It is concentrated in the micropegmatite.

Refractive index, n_z, on biotite in samples S-31 and S-32 are 1.648 and 1.647, respectively, which corresponds to the approximate

composition $K(Mg_{1.0}Fe_{1.0})AlSi_3O_{10}(OH)_2$ (Troger, 1971). The reddish color may imply a titaniferrous variety.

Secondary biotite is common in the chill zone and areas of extensive alteration.

Accessory Minerals, Chlorite, Epidote, Apatite, and Sphene

Chlorite is a wide spread alteration product that takes various forms depending upon the mineral it has replaced. Where it is a pseudomorph after clinopyroxene it forms distinct crystals that enclose exsolved granules of sphene. Orthopyroxene alters to a dull green variety or combinations of chlorite and talc. Extensive deuteric alteration of the ferromagnesians produces a poorly crystalline mat-like chlorite. The chlorite is generally pleochroic green with an anomalous blue interference color.

Epidote is recognized as a pleochroic yellow green mineral with high third order birefringence which occurs in tabular subhedra or anhedra. It crystallizes within the micropegmatite. In stage III pods, epidote has a granular habit in obvious replacement of large plagioclase laths.

Apatite is a minor accessory which forms slender needles. It is concentrated in quartz.

Sphene is a secondary mineral of two origins. In areas of intense alteration it is a reaction product in the breakdown of plagioclase and ilmenite, the latter which it fringes. It is also an exsolution product in the conversion of pyroxene to chlorite where it forms as minute blebs concentrated in fractures or along the (100) parting of remnant pyroxene.

CHAPTER V

VARIATION WITH HEIGHT IN THE INTRUSION

It is instructive to discuss the variation with height in the sill under a single heading. These changes result from the assimilation and concomitant contamination of the diabase by the above-mentioned types of xenoliths. In some examples it is possible to ascribe the variation to a particular type of inclusion, but in others the mutual interaction of dolomite, quartzite, and diabase preclude the identification of the reaction or process that has modified the diabase. In these cases only the inferred or probable influences are discussed. The prime complicating factor appears to be the opposing processes of silication and desilication by the quartzite and dolomite xenoliths respectively.

Grain Size

Variation in grain size for four mineral species from the Dawson Pass section are given in Figure 10 and Table 2. Data were obtained by measuring the apparent maximum dimension of individual crystals in thin section. Although the size measured by this method is a minimum for the largest grain size existing in the rack, the relative size differences, regardless of difficulties, probably hold.

Three contrasting behaviors are depicted in Figure 10. The opaques (excluding pyrite) and groundmass pryoxenes rapidly increase in size from the lower chill margin and thereafter remain constant throughout the upper reaches of the lower diabase. The amphibole similarly increases in size from the margin until a maximum is reached at approximately the 12 meter level in the sill. Thereafter grain size decreases

Table 2. Grain Size Distribution in the Dawson Pass Section

Sample # & elevation	OPQ	CL PYX	HB	OPX
S-46 19.2 m	0.20 mm	0.09 mm	0.50 mm	0.75 mm
S-45 16.2 m	0.21	0.09	0.61	0.66
S-44 12.2 m	0.21	0.09	0.65	----
S-43 8.8 m	0.19	0.10	0.52	----
S-42 4.6 m	0.18	0.09	0.44	----
S-41 0.9 m	0.05	0.07	0.14	----
Probable error*	0.01	0.01	0.03	0.03

Abbreviations: OPQ, opaques; CL PYR, groundmass clinopyroxenes; HB, hornblende; OPX, orthopyroxene. * as determined by duplicate analyses.

Base of granophyre at 19.8 m.

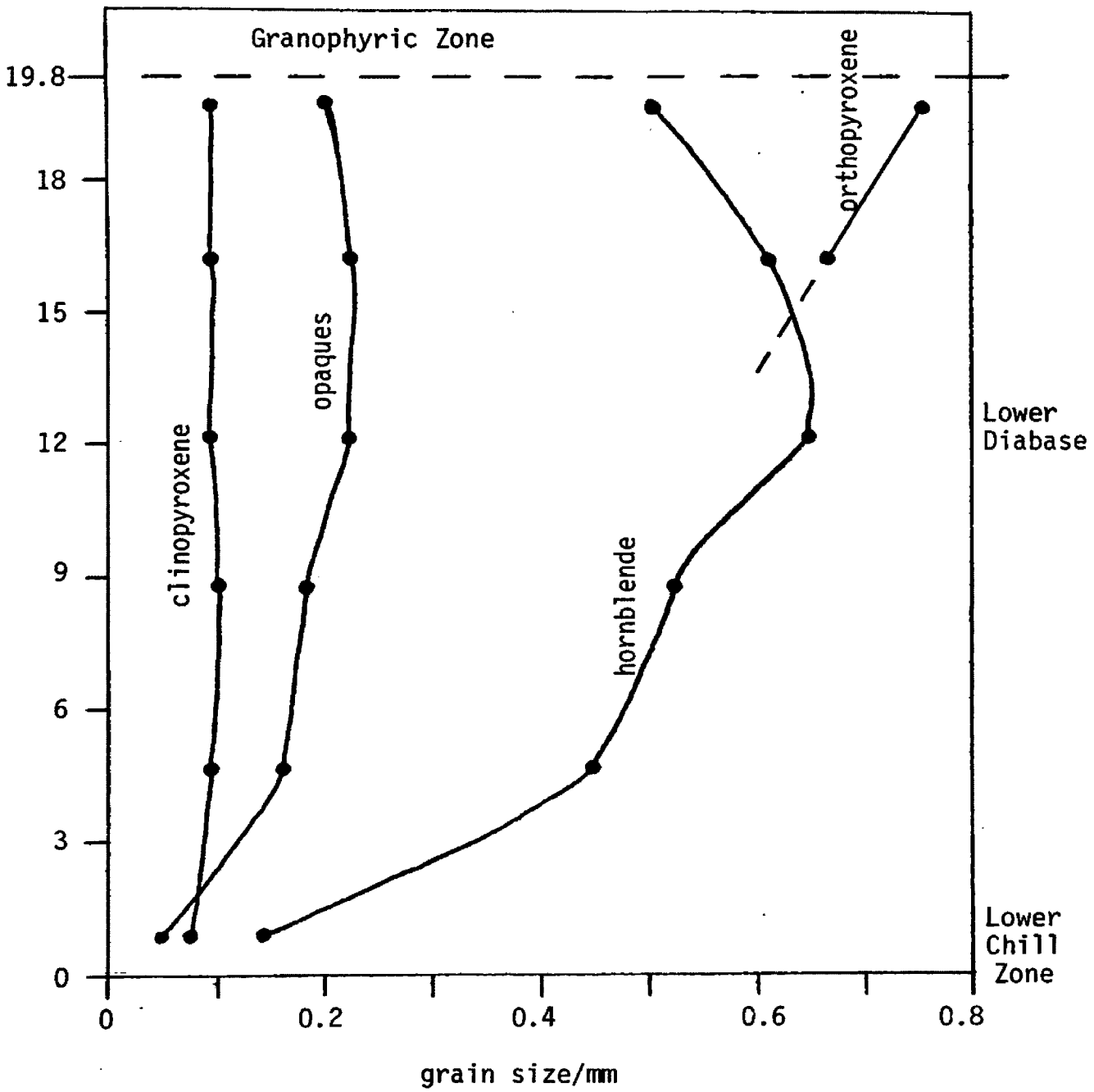

Figure 10. Grain size variations in the Dawson Pass section. Graph is based on the average of 400 measurements for clinopyroxenes and opaques and 200 for hornblende and orthopryoxene.

toward the granophyre. The limited data for orthopyroxene indicates a continuous increase in grain size up to the diabase-granophyre junction.

The dimensions of a given crystal are a function of a number of factors. Among them are the rate of nucleation and crystallization, the available time, presence of volatile medium for diffusion, and availability of essential ionic constituents. However, the three behavior patterns are compatible with a simple model.

It is believed that in the Purcell Sill the time available for crystallization was the dominant factor in controlling grain growth. Factors which acted to reduce the time of crystallization of the diabase limited the grain size of the minerals. As shown in Chapter VI, reactions involving the dolomite xenoliths release CO_2, and presumably most of this volatile was liberated in the upper reaches of the lower diabase. The addition of CO_2 to a hydrous magma increases the pCO_2 which in turn raises the solidus temperature of the mineral phases (Wyllie and Tuttle, 1959; Millhollen, 1971). This serves to abruptly limit the time for crystallization, and in the case of hornblende, restricts its grain size. The lack of size change for the Fe-Ti oxides and clinopyroxene may also reflect this influence. This proposal is supported by the larger range in crystal sizes in samples from the 16.2 and 19.2 meter level, and the distinct bimodal distribution of hornblende at the 16.2 level.

Cooling downward from the upper contact is an equally plausible explanation for the grain size distribution. Solidification should proceed at an approximately equal rate from either contact, and therefore the maximum grain size is expected near the median plane of the sill.

The sill at Dawson Pass is 27 m thick, and as depicted in Figure 10, the maximum grain size occurs near the 14 meter level. It is probable that both the influx of CO_2 and the configuration of the sill have influenced the grain size pattern.

The variation in orthopyroxene is unlike the above minerals although its crystallization was influenced by similar conditions. However, orthopyroxene results from the contamination of diabase by quartzite xenoliths. The increase in size (and modal amount) of orthopyroxene implies that the reaction had not proceeded to completion as a constant or maximum size was not obtained as in the other minerals. This suggests that the magma was not in equilibrium with respect to the influx of SiO_2 from the quartzite xenoliths.

Density

Values for rock density for the Siyeh Pass section are given in Table 3. They represent the average of two trials on each of two or three 400 g fractions from a given specimen. Although the measurements are accurate to the third decimal point, two are listed because of the compositional variations inherent in the inhomogeneous granophyre fractions.

Rock densities are commonly correlated with broad chemical and mineralogical changes (Jaeger, 1964). For this reason the modes of hornblende and chlorite, minerals that are indicative of hydrous conditions and/or deuteric alteration, are included in Table 3. It appears that in the diabase, variation in rock density may be interpreted primarily as differences in the degree of alteration. This alteration is less pronounced in the upper portions of the diabase and, as

Table 3. Density Variation and Modal Hornblende and Chlorite in the Siyeh Pass Section.

Sample # & Elevation	Density	Chlorite	Hornblende
S-37 32.0 m	3.01	1.7	18.2
S-36 31.7 m	2.90	6.3	14.9
S-35 26.5 m	2.87	8.8	5.4
S-34 23.5 m	2.92	8.5	4.9
S-32 19.8 m	3.08	0.7	5.3
S-31 13.7 m	3.05	0.6	6.4
S-30 7.6 m	2.97	7.3	5.5
S-29 3.0 m	2.98	5.0	16.1
S-28 0.6 m	3.00	5.4	13.4

Granophyre boundaries at 20.2 m and 27.0 m.

See Figure 6 for sample locations.

described above, is attributed to the depression of aH_2O in the liquid phase as a result of increasing aCO_2.

The density of the granophyre provides insight into the proportions of xenoliths and diabase that were hybridized to form the zone. The density of quartzite xenoliths averages 2.61 and that of stage II dolomite xenoliths is 3.30, whereas the density of the granophyre is about 2.90. However, the alteration-free and miarolitic-free density of the granophyre must be closer to 3.00. Although this estimate is crude, it appears that the granophyre is composed of subequal amounts of quartzite and dolomite xenoliths and, from petrographic and chemical evidence, diabase.

Modal Composition

Modal analyses for the Siyeh Pass section are given in Figure 11 and Table 4a, and for comparison, those from the Ahern Pass section are presented in Table 4b. The Dawson Pass and Highline Trail sections exhibit similar modal variations. Clinopyroxene and hornblende exhibit an antithetic relation and therefore their sum is plotted in the graph. The data has been interpolated at the diabase-granophyre boundaries to express the rapid change in rock types.

Discussion of modal variations may be considered in two parts; those that occur in the lower diabase and those that occur in the transition between diabase and granophyre.

Interpretation of the modal variations in the lower diabase is complicated by the necessity to distinguish between the contributions from the differentiation of the primary magma and that from contamination. If contamination is important in the variations the interpreta-

Table 4a. Modal Mineralogy of the Siyeh Pass Section.

Sample # & Elevation	PLAG	ALK FS QTZ	PYX_{PH}	PYX_{GR}	OPX	HB	BIO	OPQ	CHL	CHL_{PYX}	EPI	APT	SPH
S-37 32.0 m	35.5	(5.4)[1]	(25.4)[2]		1.2	18.2	---	10.7	1.7	---	1.2	---	0.6
S-36 31.7 m	44.2	(15.8)	(7.7)[3]		----	14.9	---	8.8	2.0	4.3	0.9	0.6	0.8
S-35 26.5 m	41.0	(18.4)	(16.3)[3]		----	5.4	---	7.3	1.4	7.4	0.9	0.8	0.4
S-34 23.5 m	43.8	(16.6)	(15.1)[3]		----	4.9	---	8.0	2.3	6.2	0.7	0.9	0.8
S-32 19.8 m	33.4	(7.2)	2.0	30.0	10.6	5.3	2.6	7.8	0.7	---	---	0.2	0.2
S-31 13.7 m	34.1	(7.4)	2.1	31.4	7.4	6.4	3.7	6.3	0.6	---	---	0.2	0.4
S-30 7.6 m	35.5	(6.8)	2.9	29.3	5.2	5.5	---	6.2	1.2	6.1	---	0.6	0.7
S-29 3.0 m	35.1	(8.1)	2.8	21.0	3.4	16.1	---	6.2	1.4	3.6	0.9	0.1	1.3
S-28 0.6 m	38.8	(5.8)	(25.0)[2]		1.8	13.4	---	8.3	1.3	3.1	1.8	---	0.7

Abbreviations: PLAG, plagioclase; ALK FP, alkali feldspar; QTZ, quartz; PYX_{PH}, clinopyroxene phenocrysts; PYX_{GR}, groundmass clinopyroxene; OPX, orthopyroxene; HB, hornblende; BIO, biotite; OPQ, opaques; CHL, chlorite; CHL_{PYX}, chlorite pseudomorphs after pyroxene; EPI, epidote; APT, apatite; SPH, sphene.

1. Micropegmatite as alkali feldspar plus quartz.
2. Total clinopyroxene.
3. Sector-zoned clinopyroxene.

Approximately 1200 counts were made on each 6 sq. cm. thin section. Repeat analyses indicate a precision of 1 to 2% for the major rock forming minerals.

Table 4b. Modal Mineralogy of the Ahern Pass Section

Sample # & Elevation	PLAG	ALK FS	QTZ	PYX_{PH}	PYX_{GR}	OPX	HB	BIO	OPQ	CHL	CHL_{PYX}	EPI	APT	SPH
S-72 21.3 m	35.5	15.6	8.9		(15.1)[3]	---	1.2	---	8.4	1.9	6.7	6.0	1.2	---
S-71 19.8 m	36.7	15.3	8.9		(14.8)[3]	1.1	1.1	---	9.8	2.6	5.7	3.5	0.5	---
S-69 15.2 m	26.0	5.8	5.4	2.0	34.5	8.8	7.1	3.3	5.2	0.9	0.4	---	0.3	0.3
S-68 11.6 m	33.6	3.4	3.2	1.2	34.2	8.2	2.2	---	7.9	1.3	4.1	0.1	0.2	0.4
S-67 7.6 m	30.3	5.3	4.3	3.8	25.9	4.2	11.9	---	7.3	0.9	5.0	0.7	0.4	---
S-66 4.3 m	29.0	6.9	6.5	2.4	22.0	3.2	12.3	---	7.1	1.5	6.2	1.7	0.4	0.8
S-65 0.9 m	34.4	5.3	2.6		(26.3)[2]	0.7	18.1	---	6.1	0.7	3.6	0.7	0.4	1.1

Abbreviations: as in Table 4a

2. Total clinopyroxene
3. Sector-zoned pyroxene

Base of granophyric zone at 18.6 m, samples S-71 and S-72 from granophyre.

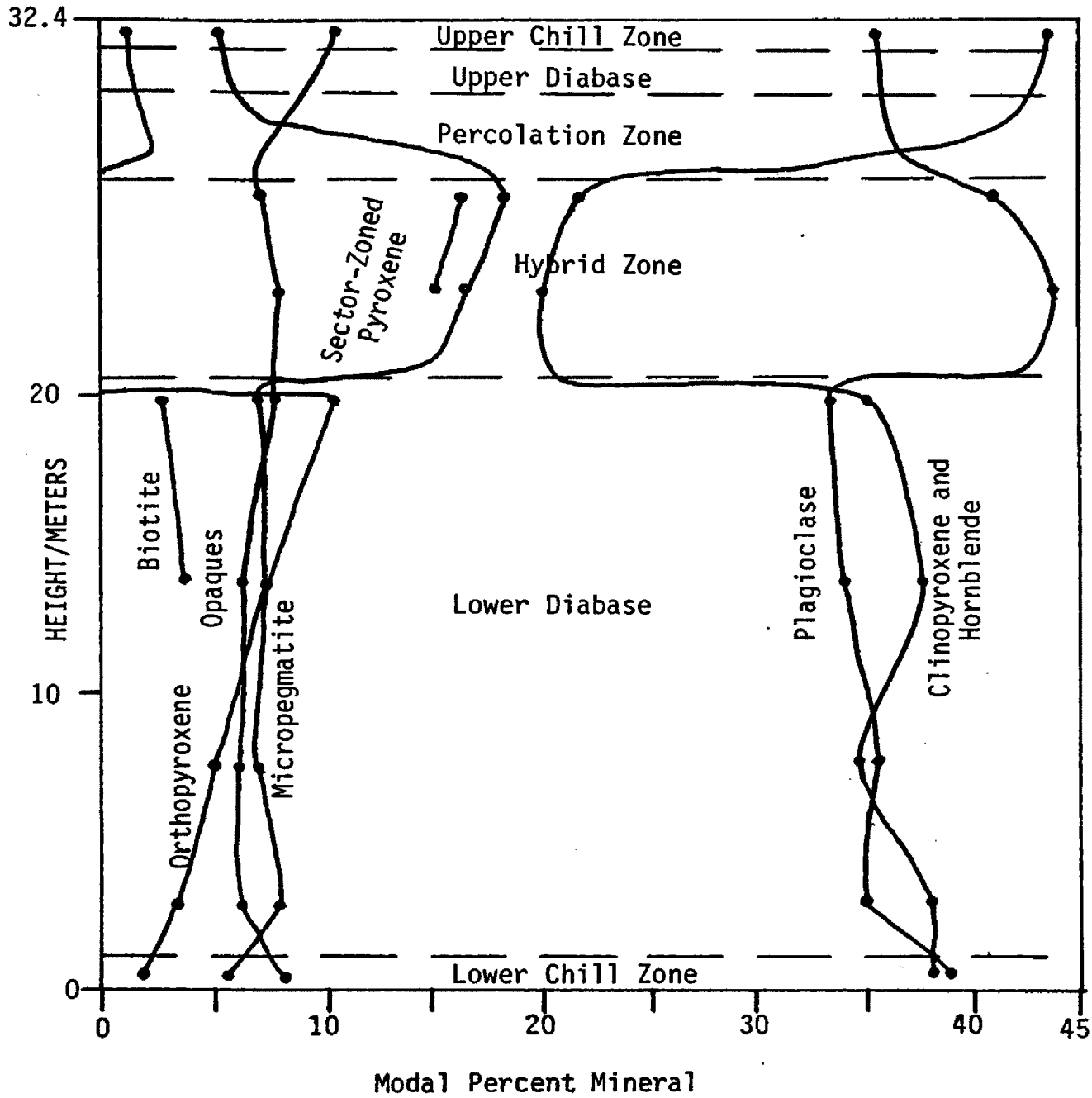

Figure 11. Modal mineralogy of the Siyeh Pass section. About 1200 counts on each 6 sq. cm. thin section. Accuracy 1-2% as determined by duplicate analyses.

tion is further complicated by the opposing influences of the two types of xenoliths and the influx or egress of elements from the melt when released or incorporated by the inclusions. The orthopyroxene trend has been discussed above and it was concluded that its appearance and modal increase may be attributed to the addition of silica to the magma by the assimilation of quartzite xenoliths. It is also thought that the variation in the other minerals was controlled by contamination. The short time for consolidation favors this conclusion (see Appendix, Cooling History) and for most parts severely limits magma differentiation. However, it does not exclude the possibility of normal differentiation being swamped by contamination. The fluctuation of micropegmatite in the diabase is consistent with the view of control of the modal profile by contamination, as quartz and alkali feldspar have been withdrawn across the quartzite xenolith boundary and enriched in the diabase. Furthermore, relatively greater or lesser amounts, as in samples S-69 and S-68 from Ahern Pass, are correlative with variations in plagioclase content. The difference in these rocks results from the resorption of plagioclase by alkali feldspar as in S-69. This is directly related to quartzite assimilation.

Noteworthy is a perceptible upward decrease in the plagioclase mode in the lower diabase in all the investigated sections (Siyeh Pass, Dawson Pass, Ahern Pass, Highline Trail, and Yarrow Creek). This is most obvious in the difference between samples from the chill zone and those immediately overlying it. Other minerals also show this type of variation. The modal changes between the chill zone and adjacent diabase indicate immediate modifications in the environment of crystallization from the intruded magma to the 'differentiated' magma.

The pyroxene-hornblende curve (Figure 11) is quite constant if this marginal change is neglected. However, if the components are inspected independently, it is apparent that they vary antithetically, with pyroxene increasing at the expense of hornblende in the less altered upper regions. The increase in the partial pressure of CO_2, thus reducing the relative partial pressure of H_2O and promoting crystallization has been forwarded to explain the reduction of grain size. It is probable that this is also responsible for the inhibition of hornblende crystallization in that the displacement of H_2O from the liquid favors the formation of the non-hydrous phase. Although biotite begins to crystallize in these upper regions the gross decrease in hornblende and chlorite more than compensate for the molecular water in biotite.

The abrupt modal variations encountered at the diabase-granophyre transition reflect the dissimilar origins of the rocks. It follows that with the addition of quartzite xenoliths the amount of micropegmatite residuum increases in the granophyre, and with additions of epidote (Ca, Al) from dolomite xenoliths and free quartz from the quartzite (or siliceous dolomite), plagioclase also increases. The pyroxene content of the granophyre is much less than that of the diabase simply because the xenoliths contain little of the pyroxene molecule. The modal distribution of the other minerals may be similarly explained by a comparison with the composition of the xenoliths.

Clinopyroxene and Orthopyroxene

Optically determined compositions of clinopyroxene and orthopyroxene are listed in Table 5 and plotted in Figure 12. The compositions are approximate, as the effects of Ti and Al substitution are unpre-

Table 5. Composition of Clinopyroxene and Orthopyroxene

Clinopyroxene

Sample # & Elevation	Optic axial angle $2V_z$	Refractive Index β	Composition
S-28 0.6 m	59°	1.693	$Ca_{49}Mg_{36}Fe_{15}$
S-29 3.0 m	57°	1.696	$Ca_{47}Mg_{34}Fe_{19}$
S-30 7.6 m	56°	1.701	$Ca_{46}Mg_{31}Fe_{23}$
S-31 13.7 m	46°	1.698	$Ca_{39}Mg_{38}Fe_{23}$
S-32 19.8 m	45°	1.693	$Ca_{38}Mg_{42}Fe_{20}$

Orthopyroxene

	Optic axial angle $2V_x$	Refractive Index γ	Composition
S-31 13.7 m	66.5°	1.700	$Ca_4Mg_{71}Fe_{25}$
S-32 19.8 m	71.4°	1.696	$Ca_4Mg_{76}Fe_{20}$

Data represent the average of six or more determinations of optical axial angles and four determinations of refractive index on each sample. Orthopyroxene compositions were cross checked by β refractive index.

See. Figure 6 for sample locations.

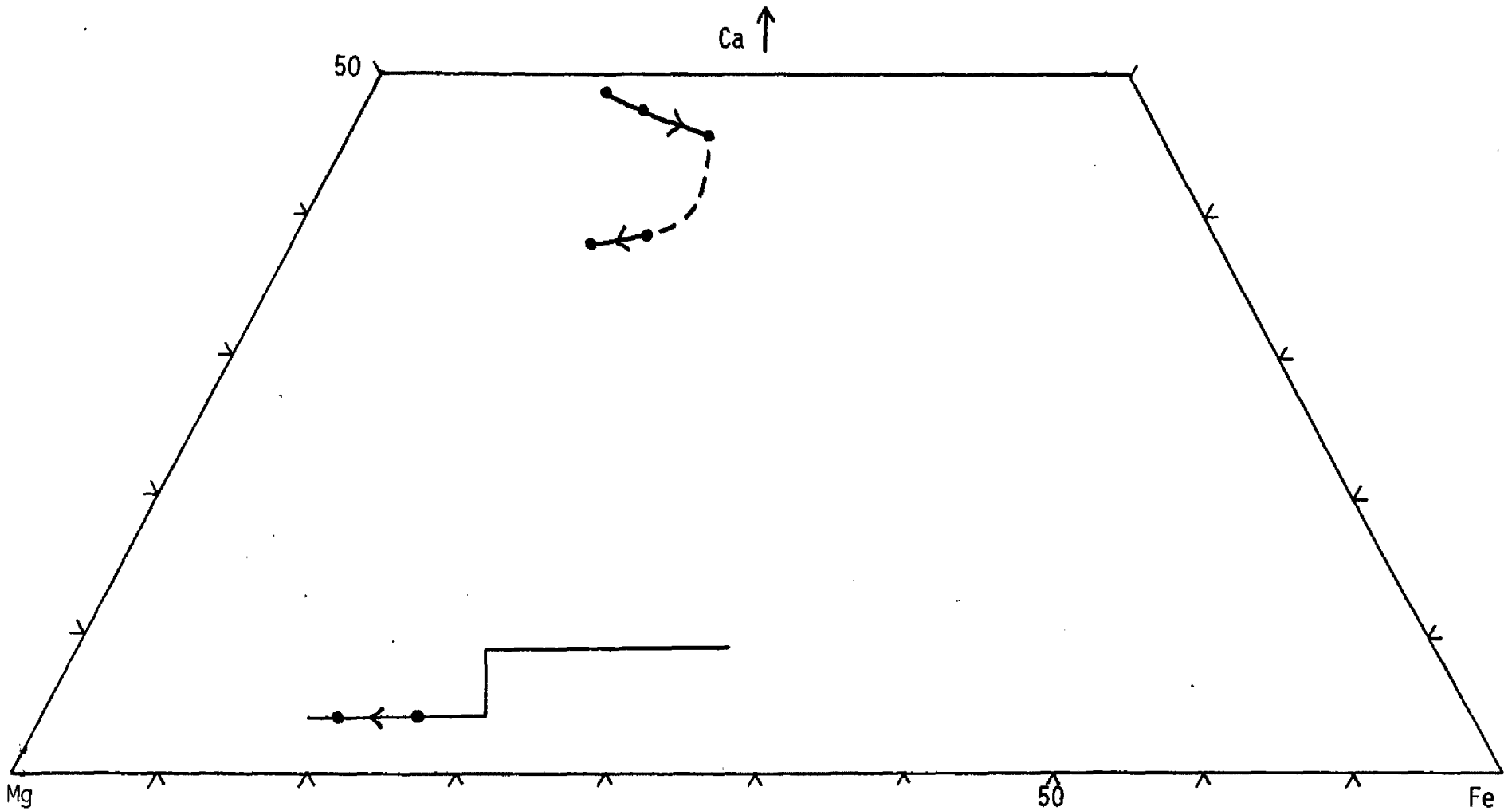

Figure 12. Variation in pyroxene composition in the Siyeh Pass section. Arrows define 'differentiation' trend. Trend dashed where uncertain.

dictable (Wilkinson, 1956, 1957). These effects may be complex because of variations induced by contamination (Le Bas, 1962). Until more exact chemical analyses are available, the following discussion is tenuous.

Samples S-28, S-29, and S-30 describe a differentiation trend typical of alkaline olivine basalts (Wilkinson, 1956) in that the crystallization path roughly parallels the diopside-hedenbergite join with minor substitution of Fe for Mg and Ca. The extensive compositional changes from S-28 to S-30 which is not found in the clinopyroxenes of alkaline olivine basalts (Murray, 1954; Wilkinson, 1956, 1957) may reflect the onset of contamination.

The clinopyroxene curve abruptly reverses direction between the 8 and 13 meter levels of the Siyeh Pass section. Mg apparently begins to substitute for Fe after a 7 mol% loss of Ca. Data from the two samples with unaltered orthopyroxene also display a trend toward Mg. It is believed that the Mg enrichment is real, as both pyroxenes follow a similar course and the interpretation of orthopyroxene composition from optical data is not complicated by variable site occupancies as is the clinopyroxenes. With respect to the Ca loss, Deer, Howie, and Zussman (1963) report that proxying of Al^{+3}, Ti^{+3}, or Fe^{+3} in tetrahedral coordination increases the optic axial angle and decreases the β refractive index, whereas if in octahedral coordination, the optic axial angle decreases and the β refractive index increases. The Purcell Sill trend is marked by a decrease in both the optic axial angle and β refractive index and therefore may not be assigned to a simple monoelemental substitution but does not negate the possibility of a coupled substitution.

The break in the pyroxene curve occurs at an equivalent level as the CO_2 induced phenomena. However, a rise in the solidus of a mineral, at a given temperature, crystallizes lower temperature, more Fe-rich phases. The observed trend is compatible with the known data if it is assumed that crystallization of the pyroxenes in S-31 and S-32 occurred at higher or equivalent temperatures than S-29 and S-30. This is possible if the pyroxenes had not begun to precipitate before the appearance of CO_2. The diabase was necessarily semi-liquid at this stage, as xenoliths migrated through it to collect as a granophyric layer. An increase in pCO_2:pH_2O would induce crystallization at these higher temperatures.

Alternatively, cooling inward from the upper contact would result in the crystallization of higher temperature assemblages. S-32 would crystallize before S-31, and therefore result in a greater Mg:Fe in the pyroxenes. The cooling history of the sill (see Appendix) has been computed to reflect this possibility. It is thought that the introduction of CO_2 and the solidification pattern were involved in these compositional variations.

Wilkinson (1956) and Tilley (1950) suggest that the difference between the pyroxene trend of the alkaline olivine basalts and that of the tholeiitic basalts depends on the crystallization of orthopyroxene. Orthopyroxene (or olivine and SiO_2) reacts with the calcic pyroxene forming augite. In this sense, the trend described by samples S-31 and S-32 may be correlated with that of tholeiitic basalts. The lag in the pyroxene composition to reflect this change may be possibly due in part to a gradual increase in $aSiO_2$ (Carmichael, Nicholls and Smith, 1970) either from the ever-increasing assimilation of SiO_2 or from a

rise in fO_2 from the dissociation of CO_2 (Nokleberg, 1973). The magnitude of this latter process in the abasnce of fO_2 buffer data is speculative.

The increase in modal pyroxene which should result from a lowering of its Ca content is not apparent in any of the samples along the length of the sill. It is likely that this increase of available CaO was extracted by the plagioclase crystallizing at higher temperatures, thus resulting in no modal variations for either plagioclase or pyroxene.

CHAPTER VI

CHEMISTRY

Diabase-Xenolith Reactions

Variations in the sill described in the previous section are attributed to the contamination of the diabase by rocks presumably incorporated during intrusion. The distribution of elements in the sill may also be explained by this mechanism, and it appears that this exerted the primary control in diabase 'differentiation'. Although differentiation in the proper sense probably occurred, it failed to produce visible effects as it was overshadowed by the chemical exchanges between diabase and xenoliths.

The Altyn Limestone (dolomite) is the most likely candidate for the parent of the dolomite xenoliths, and a whole rock analysis, from Daly (1912, p. 60) and Ross (1959, p. 55) is included in Table 6. The stratigraphic thickness of the exposed Altyn in Glacier Park is roughly 2000 feet (Ross, 1959) and variations are to be expected in its chemistry. However, the formation is essentially a magnesian limestone, with some more silicious and possibly argillaceous fractions. It may be used as a reference point for calculations regarding diabase-xenolith reactions. Analyses for stage II xenoliths (DX 3C, DX 5) and a stage III type (S-3) are given in Table 6. The stages I, II, and III are thought to represent advancing chemical and mineralogical equilibria in the dolomite.

An examination of the analyses shows that the inclusions are modified in the direction of the host rock. This encompasses additions of SiO_2, Al_2O_3, and Fe_2O_3. The xenolith has returned CaO, MgO, and CO_2

Table 6. Xenolith and Altyn Limestone Compositions

	DX-1	DX-13	DX-10	DX-12	DX 3C	DX-5	S-3	14050	1322
SiO_2	68.55	74.91	74.72	72.83	38.68	46.87	45.73	18.85	13.46
TiO_2	0.47	0.44	0.54	0.45	1.03	1.21	2.95	0.06	n.d.
Al_2O_3	13.32	12.92	14.70	13.92	19.37	13.86	13.84	1.90	1.56
Fe total as FeO	3.61	2.26	2.74	3.01	14.89	16.76	12.55	0.84	1.53
MgO	1.89	1.23	1.49	1.52	3.03	5.79	5.79	16.36	17.81
CaO	4.39	2.03	2.07	3.02	20.47	14.28	16.21	23.79	25.08
Na_2O	9.63	7.50	2.80	3.31	n.d.	1.41	n.d.	0.18	0.28
K_2O	0.10	0.18	2.43	2.71	0.35	0.34	1.26	1.06	1.08
CO_2	n.d.	n.d.	n.d.	n.d.	n.d.	n.d.	n.d.	36.65	38.08
	101.96	101.47	101.49	100.77	97.82	100.52	98.33	99.69	98.88

1. From Ross, 1959, p. 55
2. From Daly, 1912, p. 58

n.d. Not determined.

DX-1, DX-13, albite-quartz xenoliths; DX-10, DX-12, albite-alkali feldspar-quartz xenoliths; DX-3C, pryoxene-hornblende-epidote stage II xenolith; DX-5, albite-quartz-hornblende-epidote stage II xenolith; S-3, stage III dolomite xenolith; ID-14050, 1322, Altyn Limestone.

to the magma. Evidence also suggests that Na_2O was concentrated in the xenoliths. Most of these exchanges probably occurred during the prograde reactions.

Initial metamorphism of the dolomite, represented by stage I xenoliths, characteristically occur in dike exposures and have had limited time for equilibration. The principle mineral is epidote which occurs as a monomineralic aureole around a magnesian calcite. Epidote is considered a retrograde product of grossularite. In rare cases a thin erratic 1 to 4 mm zone of grossularite locally separates the calcite and epidote. Grossularite, in contact with calcite, may also be randomly dispersed throughout the outer edges of the calcite core. It has the appearance, as does the epidote (Figure 4a), of forming at the expense of the calcite. A possible prograde garnet-producing reaction is:

$$Al_2O_3 + 3SiO_2 + 3CaMg(CO_3)_2 \rightarrow Ca_3Al_2Si_3O_{12} + 3MgO + CO_2$$

This reaction necessitates the influx of Al_2O_3 (and ferric iron) at an early stage. Similar migrations have been reported elsewhere (Joplin, 1935; Gindy, 1953; Tilley, 1949; Butler, 1965). Free SiO_2 is present at this stage and may be derived from the xenolith or as is probable in later stages, from the diabase along an activity gradient into the inclusion. A reaction of this nature is also consistent with the upward increase of MgO in the diabase. Part of this eventually enters the diopside structure, though much of it was apparently released into the sill at this time.

Where epidote is adjacent to grossularite in the advancing retrograde reequilibration front, epidote may form by:

$$Al_2O_3 + H_2O + 2Ca_3Al_2Si_3O_{12} \rightarrow 2Ca_2Al_3Si_3O_{12}(OH) + 2CaO.$$

Stage II xenoliths are marked by the crystallization of diopside, which is concentrated toward the edge of the inclusions. Diopside may arise from the reaction:

$$2SiO_2 + CaMg(CO_3)_2 \rightarrow CaMgSi_2O_6 + 2CO_2$$

or with H_2O available (since the Purcell Sill erupted nearby to form pillow lavas), a lower temperature reaction:

$$8SiO_2 + H_2O + 5CaMg(CO_3)_2 \rightarrow Ca_2Mg_5Si_8O_{22}(OH)_2 + 3CaCO_3 + 7CO_2$$

and with increasing temperature and time:

$$2SiO_2 + 3CaCO_3 + Ca_2Mg_5Si_8O_{22}(OH)_2 \rightarrow 5CaMgSi_2O_6 + 3CO_2 + H_2O.$$

In stage II xenoliths, quartz and albite may be present. The stable assemblage is diopside, grossularite, $\pm$ quartz and albite, and is representative of the pyroxene hornfels facies.

Further modification to stage III is more properly considered as assimilation than metamorphism and is similar to an example recorded by Gindy (1953). The important reaction consists of the formation of a calcic plagioclase from grossularite:

$$2Al_2O_3 + 3SiO_2 + Ca_3Al_2Si_3O_{12} \rightarrow 3CaAl_2Si_2O_8$$

although this is simplified as large scale rearrangements are evident.

The reactions described have in common the addition of SiO_2 (and Al_2O_3) for the development of the next higher assemblage. The analysis of stage II xenoliths indicates that they have concentrated Al_2O_3 compared to the least-contaminated, chill zone diabase (19.37 vs. 12.48 wt %). This apparent migration of an element along an activity gradient

is also shown by MgO which is 3.03 wt % in the xenolith, down from approximately 16.50 wt % in the dolomite. The direction of movement of these elements is reversed as the xenolith becomes further incorporated into the diabase. In sample S-3, Al_2O_3 is reduced and MgO increased to levels more appropriate to the diabase. The activity gradient of SiO_2 remains in the direction of the xenolith. The resultant mineralogy and chemistry of S-3, although remaining high in CaO, and low in SiO_2 and MgO, is equivalent to the diabase.

Deuteric alteration and retrograde reactions are characteristically more pronounced in the xenoliths than the diabase. In stage III dolomite xenoliths this manifests itself by the saussuritization of plagioclase laths and the presence of hornblende and chlorite in place of pyroxene. Pyroxene in stage II xenoliths are rimmed by retrograde hornblende, the process more active at the margins leaving fewer and smaller cores. Xenoliths were responsible for the localization of volatiles as the minerals in the diabase are relatively unaffected. The xenoliths evolved in a volatile-rich environment which has also affected the adjacent diabase, as demonstrated by the larger grain size in the vicinity of the dolomite xenoliths.

Quartzite xenoliths show little reaction with the diabase. Xenoliths may exhibit pyroxene coronas and the crystallization of ferromagnesian minerals within the inclusion. The most profound effect on the xenolith is its solution and gradual rounding, characteristics that are typically associated when immersed in more acid magmas. Outcrops show a clear relation between the angularity of the xenolith and its mafic mineral content; those most spherical contain more ferromagnesian

minerals. The Na-rich (DX-1, DX-13) and K-rich (DX-10, DX-12) samples exhibit similar inward reorganization and outward contamination of diabase. The quartzites characteristically impart a pink halo of alkali feldspar to the adjacent diabase. Ernst (1960) suggests that the pink color is caused by minor amounts of Fe exsolved from the feldspar structure during cooling. This is consistent with iron entering the xenolith and localized about it. A broad pink halo is common around dolomitic xenoliths for the same reason. The diabase surrounding the quartzite is marked by a greater amount of modal quartz within a band 2-3 cm wide. Albitic xenoliths probably supplied Na_2O to the magma although this cannot be confirmed in the absence of diagnostic minerals and the inability to determine anorthite content.

The diabase has gained silica as is apparent from the rounding and solution of the quartzite xenoliths, and the quartz enrichment selvage around the xenoliths. The primary reaction for its introduction is:

$$SiO_2 + Mg_2SiO_4 \rightarrow 2MgSiO_3.$$

The amount of modal orthopyroxene increases nearly linearly in the lower diabase in response to the continual addition of SiO_2. This is coupled with the gain of Mg from the dolomite xenoliths as expressed by the whole rock analyses (Figure 13). The quartzite has acted as a source of silica and has little modified the diabase in other elements.

Preliminary relationships suggest that the quartzite xenoliths have maintained a limited miscibility with the diabase. Transfer of silica and alkalies has occurred across the rock contact, most likely by solution or vapor phase transfer, yet the xenoliths retain their

integrity with the diabase even at the granophyric boundaries. Consideration of the time and temperatures at which the xenoliths were immersed indicate that this mixing process was slow (Jaeger, 1967). Recent field and experimental studies (Yoder, 1973; McBirney and Nakamura, 1974; Smith and Silver, 1975) have shown that mutual immiscibility of liquid basaltic rock and juxtaposed liquid granitic rock is not uncommon and perhaps should be expected in geologically short times. However, studies by Wiebe, 1973, and Maury and Bizouard, 1974, show that assimilation and the homogenizing of contrasting rock types may occur in some cases. It appears that a particular set of circumstances such as differences in chemistry, notably FeO and P_2O_5 (Aniruddha, 1974) or physical properties such as viscosity (Yoder, 1973) may be controlling factors for immiscibility. Further investigations on the xenoliths in the Purcell Sill may aid in clarifying these conditions.

Whole Rock Chemistry

Whole rock chemical analyses are presented in Table 7 for samples from Siyeh Pass. Samples S-47 and S-48 from the granophyric zone of Dawson Pass indicate the inhomogeneity of small volumes of rock. Data for the contiguous diabase to granophyre sequence is shown in Figure 13. The element variations are clearly correlative with xenolith assimilation.

It is concluded that the primary influence of the quartzite xenoliths was to act as a silica-pool. Although silica was drawn into the magma this is not reflected in the whole rock chemistry as silica content remains at 48 to 49 wt % throughout the diabase. This increases

Table 7. Diabase Whole Rock Compositions in the Siyeh Pass Section

	S-28	S-29	S-30	S-31	S-32	S-34	S-35	S-47	S-48
SiO_2	48.92	48.66	48.87	49.38	48.82	51.06	50.70	50.70	52.27
TiO_2	4.27	4.22	3.72	3.86	4.39	3.76	3.57	4.24	3.41
Al_2O_3	12.50	12.09	11.86	10.83	10.32	14.61	14.59	14.45	13.72
Fe total as FeO	11.89	12.10	13.87	11.69	12.39	12.34	12.89	12.20	12.59
MgO	7.69	7.60	9.22	9.49	9.95	4.73	4.70	5.07	4.51
CaO	9.95	10.25	8.88	10.78	10.86	7.59	7.45	8.40	8.21
Na_2O	4.92	4.14	4.08	3.18	3.22	5.82	5.07	4.80	4.58
K_2O	1.04	1.26	0.74	1.02	1.29	1.81	1.83	1.51	1.92
	101.48	100.32	101.15	100.23	101.24	101.72	100.83	101.37	101.21

Analyses are by X-ray fluorescence, except for Na_2O which are by atomic absorption. Each analysis represents the average of two analyses from separate fractions of the handspecimen. Replicate runs produce consistent results. Sample locations given in Figure 6.

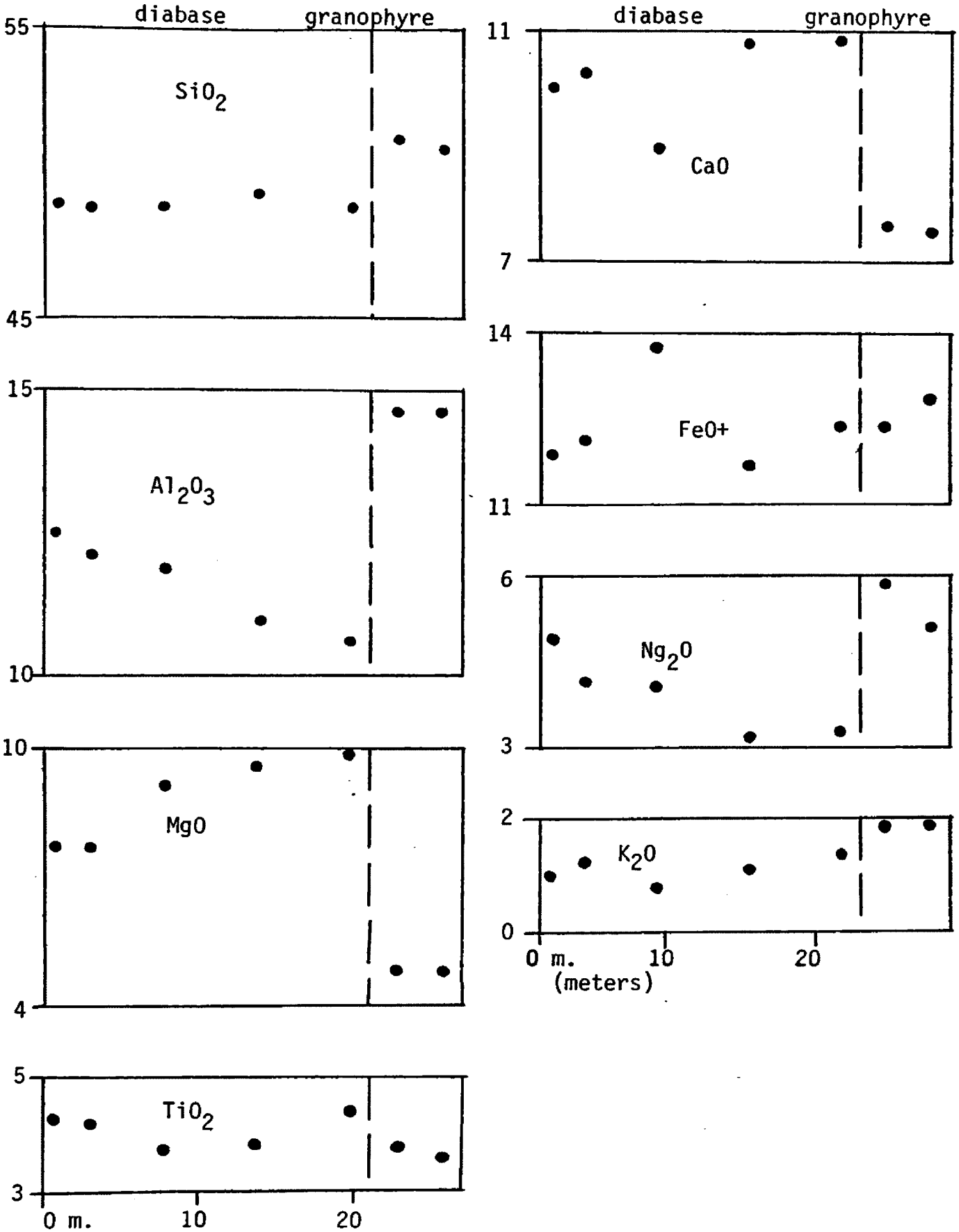

Figure 13. Diabase composition of the Siyeh Pass section.

to 51 wt % in the granophyric zone because it is partially composed of quartzite xenoliths. SiO_2 behavior in the system may be thought of in two parts; its addition into the magma from the quartzite, and removal to form Ca-Al silicates in the dolomite xenoliths. It is thought that additions and subtractions δSiO_2 were balanced and therefore the diabase acted as an intermediary receiving silica but also losing it.

Al_2O_3 shows a steady decrease in the diabase as it is incorporated into the xenoliths eventually as epidote. This linear decline demonstrates that the xenoliths reacted immediately and continuously with the magma throughout their ascent through the sill. Mg, a by-product of the grossularite-forming reaction, increases in the diabase. However, there is a lag in its distribution into the magma, the influx being first recorded from sample S-30 at the 7.6 meter level. This lag may be a sampling error, or real, and the result of inhomogeneity of the melt. For example, it is envisioned that as the xenoliths rose within the magma they reacted continuously with the adjacent diabase. The longer a xenolith remained in a given chemical environment, the greater the exchanges with the diabase. Alternatively, if the diabase lacked nearby xenoliths, its composition would be unchanged.

Fe total which should roughly parallel the decline of Al_2O_3, and is apparently concentrated in the early history of the dolomite xenoliths (compare Altyn Limestone vs. xenolith DX 3C), is anomalous.

A slight increase of CaO in the diabase may be due in part to its release from dolomite xenoliths. Alternatively, it may denote the pervasive alteration and low-grade metamorphic equilibration of

plagioclase. It was noted that the An content of plagioclase is lower than expected and there is the possibility that CaO was redistributed.

The granophyric hybrid zone is dominantly a collection of xenoliths and the rationale used in describing the modes in the zone may be applied to its chemistry. For instance, of the three rock types that compose the granophyre, only the diabase contains appreciable MgO, and therefore the MgO content of the granophyre is low. Dolomite and quartzite xenoliths are high in Al_2O_3 and accordingly there is more Al_2O_3 in the granophyre than in the diabase. The other elements express the same addition of xenoliths. The composition of the granophyric zone may be approximated using one part diabase (S-28), one part dolomite xenolith (DX 3C), and one part quartzite xenolith (DX-1, DX-10).

Composition of the Uncontaminated Magma

Three samples, two from the lower chill margin and one from the upper, were chemically analyzed and are presented in Table 8. Their normative minerals along with those from other diabase samples are given in Table 9. Samples were chosen at widely separated sections in order to determine possible lateral variations in composition. There is little difference in the samples and it is concluded that the magma was intruded rapidly and homogeneously.

The analyses indicate that the diabase has affinities with the alkaline olivine basalt family. One of the more useful compositional diagrams used to indicate broad basalt types is a plot of SiO_2 versus $Na_2O + K_2O$. When chill zone samples are plotted on such a diagram they fall well within the alkaline olivine basalt field. Classification by the CIPW norm can also be used to distinguish basalt types. Table 8

Table 8. Chill Zone Compositions

	S-28	S-41	S-80	AVG
SiO_2	48.92	48.77	49.00	48.90
TiO_2	4.27	4.05	4.27	4.20
Al_2O_3	12.50	12.36	12.58	12.48
Fe total as FeO	11.89	12.50	12.35	12.25
MgO	7.69	8.25	7.77	7.90
CaO	9.95	8.95	9.25	9.38
Na_2O	4.92	4.50	4.23	4.53
K_2O	1.04	1.66	1.47	1.39
	101.48	101.04	100.92	101.03

S-28 Siyeh Pass Section

S-41 Dawson Pass Section

S-80 Yarrow Creek Section

Table 9. CIPW Normative Minerals in the Siyeh Pass Section and Chill Zones.

	S-28	S-29	S-30	S-31	S-32	S-41	S-80
Or	6.0	7.5	4.5	6.0	7.5	9.5	8.5
Ab	27.5	26.0	36.0	27.5	25.5	25.0	29.0
An	9.5	10.5	11.5	12.3	9.8	8.5	11.3
Ne	9.0	6.9	0.3	0.9	1.8	9.0	5.1
Di	31.6	32.4	25.6	33.2	34.8	28.4	27.2
Ol	7.1	6.6	12.2	10.5	10.2	9.5	8.9
Mt	3.5	4.2	4.7	4.1	4.4	4.4	8.9
Il	5.8	5.8	5.2	5.4	6.0	5.6	5.8
	100.0	99.9	100.0	99.9	100.0	99.9	100.0

Samples S-28 through S-32 from lower diabase Siyeh Pass section.

S-41 from lower chill zone Dawson Pass section.

S-80 from upper chill zone Yarrow Creek section.

shows that all diabase samples are nepheline normative, the chill samples being more so, and therefore also indicative of alkaline olivine basalts. The very high TiO_2, which is reflected in the titaniferrous augite, implies an alkaline olivine type magma.

The presence of modal quartz appears contrary to this conclusion. In the Ahern Pass (and Dawson Pass section, data not presented) section, modal quartz increases (Table 4b) and presumably chemical analyses would verify an increase in SiO_2 wt %. Quartz enrichment in the sill along with the cited orthopyroxene reaction is consistent with assimilation of quartzite by the diabase resulting in nonequilibrium conditions.

CHAPTER VII

PETROGENESIS

The Purcell Sill diabase belongs to a basaltic province outlined by Hunt (1961). Members of the suite occur as intrusives and extrusives flanking the Rocky Mountain Trench in western Montana and southern Alberta and British Columbia. They are marked by high TiO_2 values, and it is thought that their individual characteristics were developed from combinations of fractionation and contamination. The crystallization history of the Purcell Sill, which makes up a volumetrically small fraction of the original magma, was dominated by contamination and in this way is unique in the series.

It appears that the movement of the magma through dikes was accompanied by the removal of considerable wall rock. An estimate of the amount may be made using equal parts dolomite, quartzite and diabase to form the hybrid zone. At Siyeh Pass, the hybrid zone measures 6 to 7 vertical meters of the total 32 meters of the sill. Therefore approximately 4 cubic meters of xenoliths were infused into every 28 cubic meters of diabase. Mass balance estimates involving the chemistry of the xenoliths and the influx or egress of the elements to and from the diabase are consistent with this ratio.

Xenoliths in the dikes at Cracker Lake and Otokomi Lake are exposed in relatively undigested states. In many cases they are acutely angular and have undergone limited chemical exchange with the diabase. Xenoliths of similar appearance are rare in the sill and the distinct transformations induced by xenoliths assimilation, the introduction of silica with the concomitant disappearance of olivine, and the depletion

of Al_2O_3 from the diabase are already visible in the chill zone. Such trends are amplified with further mixing, It is possible that the beginnings of assimilation preceeded intrusion.

It appears that the reactive nature of the xenoliths was promoted during and following intrusion. Xenoliths are absent from the chill margins and therefore it is postulated that a dispersive force was operative akin to that described by Komar (1972) for phenocrysts. This implies a relatively fluid magma and a high concentration of interacting xenoliths. Once in the sill environment and locked from the lower and upper chill margins, the lighter xenoliths rose. Using Stoke's Law, the calculated density values of 2.61 for quartzite, 2.76 for Altyn Limestone (less if liquid) and 2.80 for molten diabase with an average viscosity, indicates that the rise of xenoliths was rapid. In the case of the dolomite xenoliths, reaction with the diabase had increased their density to approximately 3.30 by midway in their development (stage II). Before this the grossularite-diopside inclusions may have descended in the magma. The quartzite xenoliths however were little modified and rose until bounded by the downward solidifying diabase. The preponderance of dolomite-derived inclusions in the lower diabase and the exclusion of quartzite types is attributed to this density driven process.

The upward flux of xenoliths provided a continually new and undepleted elemental environment by mixing and homogenizing. This aided in reaction and exchange with the diabase and may be contrasted with examples of contact phenomena where the composition of the intrusion has varied in a limited aureole around the contaminating rock. With other parameters constant, exchange between diabase and xenolith is

more extensive than in the absence of this movement.

An example discussed by Weibe (1973) demonstrates that significant exchange can occur in a few hours between liquid basalt and liquid granite. The migrations were favored in the Purcell Sill by mixing, the localization of volatiles around the inclusions, the dissimilarity between the xenoliths and diabase, and the apparent aggressive tendencies of the magma. The effective dissolution of the xenoliths suggests some degree of superheat in the magma. The absence of plagioclase phenocrysts and the rapid injection support this view.

The ascent of xenoliths was eventually halted by the solidified framework of the diabase cooling downward from the upper contact (Figure 6). This resulted in the collection of xenoliths and the formation of a granophyric hybrid layer. The transition zone of the upper margins of the granophyric zone is more diffuse than that of the lower contact and it appears that many of these xenoliths were trapped after flow differentiation. The lower contact of the granophyric zone is sharp, as the assembled xenoliths were able to float on the still-liquid diabase. The homogeneity of the granophyre may be due in part to the presence of volatiles and perhaps the liquid state of the xenoliths at this time.

Cooling of the diabase was directed from the margins inward. However, solidification was delayed at the granophyric zone boundaries since its crystallization temperature was less than that of the diabase. This situation is evidenced by the percolation zone that exists above the granophyre and the deflection in the joint pattern at the upper granophyre boundary. In the percolation zone the interstitial material has been enriched by solutions high in SiO_2, K_2O and H_2O. This is

confirmed by the increase in modal quartz, alkali feldspar, resorption of plagioclase by alkali feldspar and the predominance of hornblende over pyroxene.

The pyroxene of the granophyric hybrid zone is unlike the titan-augite that is typical of the diabase, and is termed sector-zoned. Although the exact mechanism by which sectorizing is accomplished is debatable, researchers agree that its origin may be attributed to rapid crystallization (Nakamura, 1973; Nakamura and Coombs, 1973, 1973) which allows the incorporation of ions into sites otherwise unfavorable under equilibrium conditions. This suggests that the gradual crystallization of the granophyre may have been interrupted by the influx of CO_2 into the system and a consequent chilling effect. An alternative intrepretation is that the pyroxene did not nucleate until the granophyric zone was supersaturated with respect to the mineral. Growth conditions would be accelerated, resulting in sector-zoned pyroxene. The large crystal size of this layer does not belie this fact, as the hybrid zone was rich in volatiles and maintains a pegmatitic character.

It is demonstrated that assimilation of the dolomite and quartzite xenoliths influenced the diabase in contrasting ways. Dolomite xenoliths are responsible for large-scale exchanges of the oxides Al_2O_3, MgO, SiO_2, and possibly Fe_2O_3. These variations have not greatly altered the modes of the sill and it is probable that these changes are reflected in the compositions of individual mineral phases. The advent of CO_2 on the crystallizing diabase effected more rapid solidification with smaller grain size, higher temperature assemblages, and favored the production of non-hydrous minerals.

The solution and incorporation of quartzite has affected the modal assemblages. These include the formation of orthopyroxene and the presence of free quartz.

REFERENCES

Aniruddha, D., 1974, Silicate liquid immiscibility in the Decan Traps and its petrogenetic significance; G.S.A. Bull., v. 85, p. 471-474.

Butler, B.C.M., 1965, Epidiorite-limestone contact relations at Burawai, Hazara District, West Pakistan: Mineral. Mag., Tilley volume, v. 34, p. 82-91.

Carmichael, I.S.E., Nicholls, J., and Smith, A.L., 1970, Silica activity in igneous rocks: Am. Mineral., v. 55, p. 246-263.

Daly, R.A., 1912, Geology of the North American Cordillera at the forty-ninth parallel: Canada Dept. of Mines and Geol. Surv. Mem. # 38, Part I, Chapter IX, 50-65, p. 207-220.

Deer, W.A., Howie, R.A., and Zussman, J., 1963, Rock Forming Minerals, v. 2: Chain silicates: John Wiley and Sons, Inc. New York, p. 132.

Ernst, W.G., 1960, Diabase, Granophyre relations in the Endion Sill, Duluth, Minnesota: Jour. Petrol., v. 1, p. 286-303.

Eslinger, E.V., and Savin, S.M., 1973, Oxygen-Isotope Geothermometry of Burial Metamorphic Rocks of the Precambrian Belt Supergroup, Glacier National Park, Montana: G.S.A. Bull., v. 84, p. 2549-2560.

Finlay, G.I., 1902, Igneous rocks of the Algonkian Series; in Stratigraphy and structure, Lewis and Livingston Ranges, Montana: Geol. Soc. Amer. Bull., v. 13, p. 349-352.

Gindy, A.R., 1953, Progressive replacement of limestone inclusions in granite at Ballynacarrick, Co. Donegal: Geol. Mag., v. 90, p. 152-158.

Hunt, G.H., 1958, Petrology of the Purcell Sills in the St. Mary Lake area, British Columbia: Unpublished M.S. thesis, University of Alberta, 52 p.

_____, 1961, The Purcell eruptive rocks: Unpublished Ph.D. dissertation, University of Alberta, 139 p.

Jaeger, J.C., 1957, The temperature in the neighborhood of a cooling intrusive sheet: Am. J. Sci., v. 255, p. 306-318.

_____, 1964, The value of measurements of density in the study of dolerites: Geol. Soc. of Australia Jour., v. 11, part I, p. 133.

_____, 1967, Cooling and solidification of igneous rocks: in Basalts: the Poldervaart treatise of rocks of basaltic composition, ed. by H.H. Hess, and A. Poldervaart: John Wiley and Sons, Inc. New York, v. 2, p. 503-536.

Joplin, G.A., 1935, Diorite Limestone reaction at Ben Bullen, New South Wales: A study in contamination; Geol. Mag., v. 72, p. 97-116.

Komar, P., 1972, Mechanical interactions of phenocrysts and flow differentiation of igneous dikes and sills: Geol. Soc. Amer., v. 83, p. 973-988.

Le Bas, M.J., 1965, The contamination of a gabbro by carboniferous limestone at Carlingford, Co. Louth: Mineral. Mag., Tilley volume, v. 34, p. 292-302.

McBirney, A.R., and Nakamura, Y., 1974, Immiscibility in late-stage magmas of the Skaergaard Intrusion: Annual Report of the Director Geophysical Laboratory, p. 348-352.

Maury, R.C., and Bizouard, H., 1974, Melting of acid xenoliths into a basinite: An approach to the possible mechanism of crustal contamination; Contr. Min. and Petrol., v. 48, p. 275-286.

Millhollen, G.L., 1971, Melting of nepheline syenite with H_2O and H_2O + CO_2 and the effect of dilution of the aqueous phase on the beginning of melting: Am. J. Sci., v. 270, p. 244-254.

Murase, T., and McBirney, A.R., 1973, Properties of some common igneous rocks and their melts at high temperatures: Geol. Soc. Amer. Bull., v. 84, p. 3563-3592.

Murray, R.J., 1954, The clinopyroxenes of the Garbh Eilean Sill, Shiant Isles: Geol. Mag., v. 91, p. 17-31.

Nakamura, Y., 1973, Origin of sector-zoning of igneous clinopyroxenes: Am. Mineral., v. 58, p. 986-990.

_____, and Coombs, D.S., 1973, Clinopyroxenes in the Tawhiroko tholeiitic dolerite at Moerake, North-Eastern Otago, New Zealand: Contr. Min. and Petrol., v. 42, p. 213-228.

Nokleberg, W.J., 1973, CO_2 as a source of oxygen in the metasomatism of carbonatites: Am. J. Sci., v. 273, p. 498-514.

Ross, C.P., 1959, Geology of Glacier National Park and the Flathead Region Northwestern Montana: U.S. Geol. Surv. Prof. Paper 296.

Slemmons, D.B., 1962, Determination of volcanic and plutonic plagioclases on a three- or four-axis universal stage: Geol. Soc. Amer. special paper 69.

Smith, D., and Silver, L.T., 1975, Potassic granophyre associated with Precambrian diabase, Sierra Ancha, Central Arizona; G.S.A. Bull., v. 86, p. 503-513.

Spry, A., 1961, The origin of columnar jointing, particularly in basalt flows: Geol. Soc. Australia Jour., v. 8, p. 191-216.

Tilley, C.E., 1949, An alkali facies of granite at granite-dolomite contacts in Skye: Geol. Mag., v. 86, p. 81-93.

Tilley, C.E., 1950, Some aspects of magmatic evolution: Geol. Soc. Lond. Quart. J., v. 106, p. 37-61.

Troger, W.E., 1971, Optische Bestimmung der gesteinsbildenden Minerale: E. Schweizerbart'sche Verlagsbuchhandlung, Stuttgart, p. 62, 107.

Turner, F., and Verhoogen, J., 1960, Igneous and Metamorphic Petrology: McGraw-Hill Book Co., New York, 694 p.

Weibe, R.A., 1973, Relations between coexisting basaltic and granitic magmas in a composite dike: Am. J. Sci., v. 273, p. 130-151.

Wilkinson, J.F.G., 1956, Clinopyroxenes of alkali olivine-basalt magma: Am. Mineral., v. 41, p. 724-743.

_____, 1957, The clinopyroxenes of a differentiated teschenite sill near Gunnedah, New South Wales: Geol. Mag., v. 94, p. 123-134.

Wyllie, P.J., and Tuttle, O.F., 1959, Effect of carbon dioxide on the melting of granite and feldspars: Am. J. Sci., v. 257, p. 648-655.

Yoder, H.S., Jr., 1973, Contemporaneous basaltic and rhyolitic magmas: Am. Min., v. 58, p. 153-171.

APPENDIX A

COOLING HISTORY

The assumed physical parameters used to calculate the cooling of the sheet by the method of Jaeger (1957, 1967) are listed below.

Case I Temperature range of solidification of magma:

$T_1 = 1200°C$, $T_2 = 750°C$

Case II Temperature range of solidification of magma:

$T_1 = 1200°C$, $T_2 = 950°C$

Density of solidified basalt: = 3.00

Density of liquid basalt: = 2.72

Thermal conductivity of solidified magma: $K_1 = .0032$

Thermal conductivity of liquid magma: $K_2 = .0032$

Specific heat of solidified magma: $C_1 = .025$

Specific heat of liquid magma: $C_2 = .030$ (Plus latent heat)

Values for specific heat and latent heat are from Jaeger (1957, 1967), liquid basalt density and thermal conductivity are from Murase and McBirney (1973). Density of the chilled margin was measured. Two temperature ranges were assumed, 1200°-750°C for complete crystallization of a water-rich magma, and 1200°-950°C for crystallization of plagioclase and pyroxenes which would effectively prevent further ascent of xenoliths (Turner and Verhoogen, 1960). Time for solidification to a given plane is presented below and in Figure 6.

	Case I	
Sample	S-29 at 3.0 meters	2.1 years cooling interval
	S-30 7.6	5.2
	S-31 13.7	9.5
	S-32 12.6	8.7 (cooling from upper contact)
	Case II	
Sample	S-29 at 3.0 meters	0.95 years cooling interval
	S-30 7.6	2.4
	S-31 13.7	4.3
	S-32 12.6	3.9 (cooling from the upper contact)

Little trapping of xenoliths is evident, which implies that the allowable time for diffusion and reaction was controlled by the rise of xenoliths rather than strict cooling and solidification of the sill. If this is true, factors governing the rise and/or fall of xenoliths need to be considered. Data for basalt magma viscosities, especially in the presence of volatiles, are scant and open to question. Employing suggested basalt viscosities in Stoke's Law gives times for xenolith-diabase reactions significantly less than for solidification. Factors such as accelerated crystallization by increases in CO_2, and the heat lost to the xenoliths complicate the issue. Nevertheless, the above calculations are of the right order of magnitude and emphasize the short reaction times.

APPENDIX B

COLLECTION SITES

Ahern Pass: at Ahern snow drift, between Ahern Pass and Granite Park.

Cracker Lake: dike at head of Cracker Lake.

Dawson Pass: between Dawson Pass and Flinsch Peak on Continental Divide.

Fifty Mountain: west of Cathedral Peak, off trail to Fifty Mountain Camp.

Highline Trail: northwest of Haystack Butte above the trail. Sill transgresses Highline Trail approximately 1 km from Logan Pass.

Highway 2: up unnamed creek near Nimrod.

Otokomi Lake: dike at head of Otokomi Lake in Roes Basin.

Siyeh Pass: on Metahpi Peak ridge leading down to Siyeh Pass.

Scalplock Mountain: on trail near top of Scalplock Mountain.

Yarrow Creek: south slope of Spionkop Ridge, 14 miles north of international boundary.